NEWGENESS

Pre-normative recommendations for the system-based direct design of stainless steel frames using advanced analysis.

Itsaso Arrayago, Kim J.R. Rasmussen,
Hao Zhang, Esther Real

European Commission

Marie Skłodowska-Curie Actions
Research Fellowship Programme

UNIVERSITAT POLITÈCNICA DE CATALUNYA
BARCELONATECH

THE UNIVERSITY OF SYDNEY

VISIT
newgeness.com
FOLLOW
@newgeness

ACKNOWLEDGEMENTS

The project leading to this document has received funding from the European Union's Horizon 2020 Research and Innovation Programme under the Marie Sklodowska-Curie Grant Agreement No. 842395 (NewGeneSS project).

INDEX

FOREWORD

The research project NewGeneSS, the acronym of "NEW GENEration design methods for Stainless steel Structures" was financed by the European Union's Horizon 2020 Research and Innovation Programme under the Marie Sklodowska-Curie Actions (2018). The NewGeneSS project aimed at developing the basis of system-based direct design approaches for stainless steel structures in the European framework by calibrating suitable system safety factors from rigorous structural reliability considerations, and at delivering the pre-normative design recommendations included in this document.

The NewGeneSS project involved two academic partners, Universitat Politècnica de Catalunya (UPC) and the University of Sydney, in addition to a design office in which a Secondment was conducted. The researchers involved in the project were:

- Dr. Itsaso Arrayago – Universitat Politècnica de Catalunya (UPC)
- Prof. Kim J.R. Rasmussen – The University of Sydney
- Assoc. Prof. Hao Zhang – The University of Sydney
- Prof. Esther Real – Universitat Politècnica de Catalunya (UPC)

In addition to the development of the pre-normative design recommendations reported in this document, the different research works carried out in the project and the corresponding outcomes have been published in several journal papers and conference articles, which have been published in Open Access and are accessible for free. A list of these publications, with the corresponding access links, is provided herein, in which additional information to that detailed in this document can be found. Apart from these publications, the NewGeneSS project has produced other output materials for the communication and dissemination of the results, including recorded webinars in English and Spanish, a set of workshops in different design offices and a series of workshops for academics in several universities across Europe.

Journal papers:

- Arrayago I., Rasmussen K.J.R. and Real E. Statistical analysis of the material, geometrical and imperfection characteristics of structural stainless steels and members. *Journal of Constructional Steel Research* 175, 106378, 2020.

- Arrayago I. and Rasmussen K.J.R. System-based reliability analysis of stainless steel frames under gravity loads. *Engineering Structures* 231, 111775, 2021.
- Arrayago I., Rasmussen K.J.R. and Zhang H. System-based reliability analysis of stainless steel frames subjected to gravity and wind loads. *Structural Safety* 97, 102211, 2022.
- Arrayago I. and Rasmussen K.J.R. Reliability of stainless steel frames designed using the Direct Design Method in serviceability limit states. *Journal of Constructional Steel Research* 196, 107425, 2022.
- Arrayago I. and Rasmussen K.J.R. Influence of the imperfection direction on the ultimate response of steel frames in advanced analysis. *Journal of Constructional Steel Research* 190, 107137, 2022.
- Arrayago I., Zhang H. and Rasmussen K.J.R. Simplified expressions for reliability assessments in code calibration. *Engineering Structures* 256, 114013, 2022.

Conference articles:

- Arrayago I., Rasmussen K.J.R. and Real E. Statistical data for system-based reliability analysis of stainless steel structures with hollow sections. *c/e papers Special Issue: EUROSTEEL 2021 Sheffield — Steel's coming home* 4 (2-4), 1565–1574, 2021.
- Arrayago I., Rasmussen K.J.R., Zhang H. and Real E. Direct design of stainless steel frames: recommendations and case studies. *c/e papers Special Issue: SDSS 2022* 4(5), 506–514, 2022.
- Arrayago I., Rasmussen K.J.R., Zhang H. and Real E. On the development of the system-based direct design approach for stainless steel frames using advanced analysis. *Proceedings of the Sixth International Experts Seminar on Stainless Steel in Structures*. London, United Kingdom, 2022.

Webinars:

- New system-based direct design methods for steel structures (in English).
- Nuevos métodos de cálculo directo basados en sistemas para estructuras de acero (in Spanish).

It is important to highlight that this document focuses on cold-formed stainless steel structures but would be generally applicable to different types of steel structures with a few modifications on aspects related to the constitutive equations used to describe the response of the material and the models adopted for residual stresses. The document and its content have been shared and discussed with experienced practicing engineers to guarantee ease of use and maximize its acceptance from professionals in the future. Furthermore, the pre-normative design recommendations have been developed in such a way that, despite the uncertainties concerning the future of the code recommendations, its content is as aligned as possible with the provisions given in prEN 1993-1-14.

September 7th, 2022

Itsaso Arrayago and co-authors

1. INTRODUCTION

1.1. SYSTEM-BASED DIRECT DESIGN METHODS USING ADVANCED ANALYSIS

Current international specifications for the design of steel and stainless steel structures consider the traditional member-based *two-step* design approach, in which structural systems are considered as a set of individual members and connections whose resistance needs to be checked based on the design equations prescribed in the standards against the design loads determined from a prior structural analysis, usually elastic. Nevertheless, in the last years direct design approaches, in which the resistance of a structural member, a part of a structure or a complete structural system is evaluated directly from an advanced finite element (FE) analysis, are becoming more popular owing to the advances in structural analysis software. This has allowed to replace the generally time-consuming design equations predicting the resistance of structural components prescribed in standards by advanced finite element models, from which the strength of these components can be estimated directly. In this context, current international specifications for the design of steel structures such as AS/NZS 4100 [1], AS/NZS 4600 [2], AISC 360 [3] and prEN 1993-1-14 [4] already incorporate preliminary versions of different direct design methods, providing prescriptions on how advanced models should be built.

In addition to being *two-step* methods, current design approaches are member-based. This means that unless a proper global plastic analysis is carried out, traditional design methods generally assume that the capacity of the structure is reached once the resistance of the most critical component of the structure is attained (i.e., when the critical component yields or fails by instability). As a consequence of the improvements in FE software and the computational capabilities of desktop computers, it is now possible to carry out advanced FE analyses on complex and large structural systems to predict their behaviour and failure modes with great accuracy, making it possible to develop system-based approaches in which the interaction between the different structural components is fully considered and exploited. Combining direct design methods with system-based approaches, a more holistic design of steel structures is possible, which has led to the development of novel design methods such as the Direct Design Method (DDM).

Based on advanced FE models that account for all the relevant aspects that influence the behaviour of steel structures (including material and geometric nonlinearities, residual stresses, initial geometric imperfections and the actual response of connections), the characteristic R_{k} resistance of whole systems can be estimated numerically. One of the advantages of the DDM over the current member-based *two-step* design approach is that the ultimate limit state check is direct and very simple, as shown in Eq. 1, where $\gamma_{\mathrm{M,s}}$ is the system partial safety factor, γ_{i} corresponds to the load amplification factors and $S_{\mathrm{k,i}}$ are the characteristic loads.

$$\frac{R_{\mathrm{k}}}{\gamma_{\mathrm{M,s}}} \geq \sum \gamma_{\mathrm{i}} S_{\mathrm{k,i}} \qquad \text{Eq. 1}$$

Likewise, the serviceability limit state verifications can be also performed directly from the advanced FE models by checking whether the deflections and lateral displacements in the system are below the corresponding allowable deflection limits, which can be determined from structural specifications or other requirements. In addition to the simplicity in the design checks, the DDM has the advantage of being capable of fully exploiting the load redistribution capacity of redundant structures, leading to potentially more economic designs and ensuring a more uniform reliability across different structural systems [5].

Nevertheless, since these direct design methods are system-based, they require the adoption of system safety factors $\gamma_{\mathrm{M,s}}$ calibrated independently using system-based structural reliability considerations that account for the effect of the uncertainties in the resistance of systems. While most of the current design specifications include clauses on how the advanced FE models should be built, generally they do not prescribe suitable values for the system factors $\gamma_{\mathrm{M,s}}$ to be assumed when these system-based direct design approaches are adopted. Currently, these specifications only require that reliability levels equivalent or higher than those achieved with the traditional member-based *two-step* design approaches be guaranteed, without specifying how this may be done. Consequently, research efforts have focused on the development of a rigorous structural reliability framework for the calibration and recommendation of system factors for steel frames [5-8], cold-formed steel structures [9] and portal frames [10], racks [11] and scaffolding systems [12] in the ASCE and Australian design frameworks. In a similar way,

the NewGeneSS project [13] aimed at carrying out the corresponding calibrations for stainless steel structures in [14-17] and to extend the system-based direct design approach to the Eurocode design framework.

1.2. SCOPE OF THE DOCUMENT

This document is a guide for the system-based direct design of stainless steel frames using advanced analysis, and includes the pre-normative design recommendations developed within the EU-funded NewGeneSS project [13]. Considering that the reliability calibrations for system-based design of stainless steel structures in the Project were limited to structures with cold-formed elements and to load scenarios including gravity loads (dead and imposed gravity loads) and gravity plus wind loads, the system factors recommended in this document only correspond to these structure types and load cases (excluding other load scenarios that include snow, thermal or accidental actions). Many of the considerations regarding the creation of the advanced FE models are, however, applicable to a wider range of steel structural systems.

It is also worth noting that these recommendations only cover the design of stainless steel frames in the Eurocode framework, although equivalent recommendations have been also developed for the US-ASCE and Australian design frameworks in the NewGeneSS project. More information regarding these additional recommendations can be found in the original publications [15-17] and corresponding design standards (AISC 370 [18], ASCE 8 [19] and AS/NZS 4673 [20]).

This document is comprised of eleven chapters covering the system-based direct design of stainless steel frames using advanced finite element analysis, and provides guidance on how the advanced finite element models should be built, the most relevant structural features that should be taken into account, the types of structural analysis to be carried out and how design checks corresponding to Ultimate Limit States (ULS) and Serviceability Limit States (SLS) should be performed. Two case studies are also included, in which the design process using system-based direct design approaches is illustrated, and the resulting stainless steel frames are compared to those obtained using the traditional member-based *two-step* design approach.

Although some of the recommendations included in this document, especially those corresponding to the material behaviour, initial geometric imperfections and residual

stresses, are aligned with the relevant parts of Eurocode 3 (i.e., prEN 1993-1-4 [21] and prEN 1993-1-14 [4]), this document is not intended to replace such standards and users should refer to the official current versions of the Eurocode when designing stainless steel frames. This document only aims at providing guidance for the implementation, consolidation and widespread of system-based direct design approaches.

1.3. BACKGROUND TO THE PRE-NORMATIVE DESIGN RECOMMENDATIONS

The reliability framework built for the calibration of system partial safety factors is summarized in Figure 1: it is comprised by six steps and equivalent to that built to determine system factors for the direct design of steel frames in [5-12]. In addition to the different publications disseminating the background research work for these pre-normative design recommendations, which are listed in the Foreword, a detailed overview of the NewGeneSS project is also given in [22].

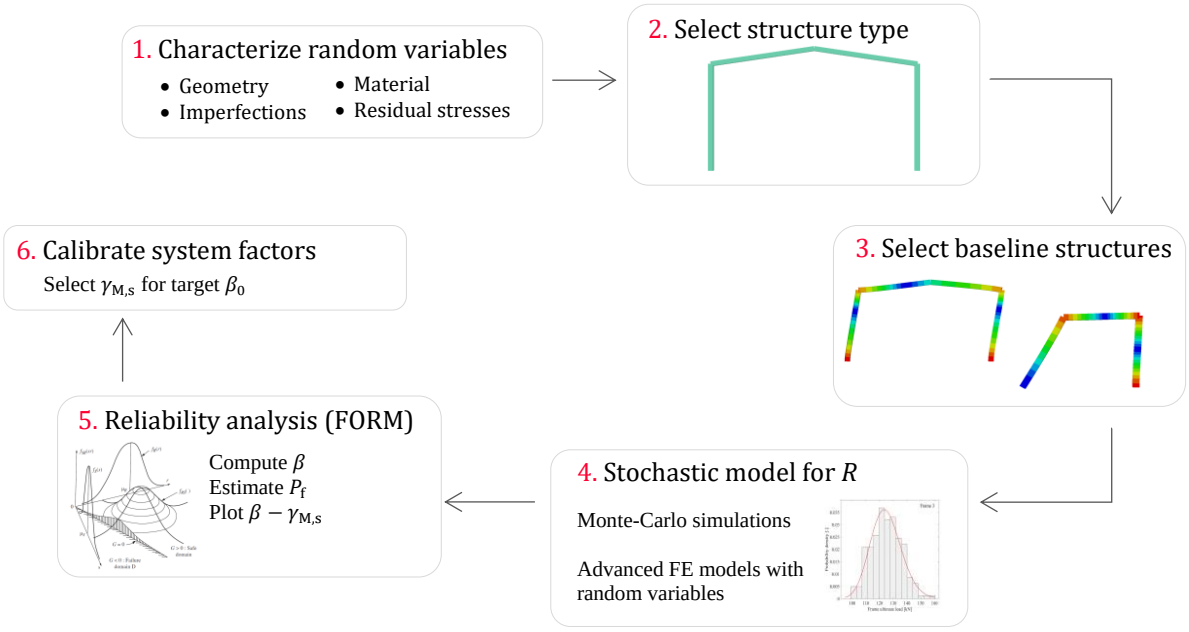

Figure 1. Reliability framework for the calibration of system factors.

A summary of the six steps comprising the reliability framework for the calibration of the system safety factors for stainless steel portal frames is as follows:

- *Step 1: Characterize random variables*. The first step was to characterize the random variables defining and influencing the response of stainless steel structures, such as geometric properties, initial geometric imperfections, material behaviour, and residual stresses. This analysis is reported in [14].

- *Steps 2 & 3: Select the structural type and baseline structures*. Then, the structural types to be analysed were selected, including the definition of representative baseline structures exhibiting different failure modes (i.e., instability, yielding-redistribution). In the NewGeneSS project stainless steel portal frames were investigated using six different baseline structures.
- *Step 4: Determine the stochastic models for the resistance of baseline frames*. Carrying out Monte-Carlo type simulations on advanced finite element models using random variables according to the characterization in Step (1), the stochastic models for the resistance R were determined for the stainless steel baseline frames when subjected to gravity loads in [15] and to gravity plus wind loads in [16].
- *Step 5: Carry out the reliability analyses*. Using the resistance distributions determined in Step (4) and the information available in the literature for the stochastic models for the different types of loads considered in [15,16], the reliability analyses can be carried out using First-Order Reliability Methods (FORM) to compute the reliability indices β, estimate the probability of failure P_{f}, and determine the $\beta - \gamma_{\mathrm{M,s}}$ relationships.
- *Step 6: Calibrate the system factors for the direct design of stainless steel frames*. Based on suitable target reliability indices β_0, the required system partial safety factors $\gamma_{\mathrm{M,s}}$ can be calibrated and recommended.

2. LOADS AND LOAD COMBINATIONS

Eurocode 1 (EN 1991) provides comprehensive information on all the actions to be considered in the design of buildings and other structures. EN 1991 is divided in four main parts, namely General Actions, Traffic loads on bridges, Actions by cranes and machinery, and Actions in silos and tanks. The first part, which is sub-divided into seven parts, covers the typical loads to be applied in building structures, including:

- EN 1991-1-1 for self-weights and imposed loads for buildings
- EN 1991-1-2 for actions on structures exposed to fire
- EN 1991-1-3 for snow loads
- EN 1991-1-4 for wind actions
- EN 1991-1-5 for thermal actions
- EN 1991-1-6 for actions during execution
- EN 1991-1-7 for accidental actions

The development of the system-based direct design method for steel structures is currently limited to frame-type structures, and in the case of stainless steel structures, to portal frames. In addition, the reliability calibrations carried out only cover the most common load cases to which frame structures are subjected, including gravity load (dead and imposed loads) and gravity plus wind load scenarios. For each type of loading case, however, calibrations have considered a wide range of imposed-to-dead and gravity-to-wind load ratios.

According to prEN 1990 [23] combinations of actions for Ultimate Limit States (ULS) should be calculated for (i) the persistent and transient (fundamental) design situations, (ii) accidental design situations, (iii) seismic design situations, and (iv) fatigue design situations. Considering that the design recommendations included in this document only refer to the persistent and transient (fundamental) design situations, the relevant combination of actions is given in Eq. 2, where F_{d} are the design values of actions, $\gamma_{\mathrm{G,i}}$ is the partial factor for permanent actions, $G_{\mathrm{k,i}}$ is the characteristic value of the permanent actions, $\gamma_{\mathrm{Q,1}}$ is the partial factor for the leading variable action, $Q_{\mathrm{k,1}}$ is the characteristic value of the leading variable action, $\gamma_{\mathrm{Q,j}}$ is the partial factor for the variable action j, $\psi_{0,\mathrm{j}}$ is the combination factor for the variable action j, and finally $Q_{\mathrm{k,j}}$ is the partial factor for

the variable action *j*. The characteristic values of the different loads (i.e., permanent loads, imposed loads, wind loads, etc.) can be obtained from the relevant parts of EN 1991, while the partial factors and combination factors for the loads are prescribed in Annex A of prEN 1990 [23].

$$\sum F_{\mathrm{d}} = \sum_{i} \gamma_{\mathrm{G,i}} G_{\mathrm{k,i}} + \gamma_{\mathrm{Q},1} Q_{\mathrm{k},1} + \sum_{j>1} \gamma_{\mathrm{Q,j}} \psi_{0,\mathrm{j}} Q_{\mathrm{k,j}} \qquad \text{Eq. 2}$$

The combination factors ψ_0 for imposed loads in buildings and wind actions, as prescribed in Annex A of prEN 1990 [23], are summarized in Table 1, while Table 2 reports the partial factors on actions for the persistent and transient design situations and structural resistance verifications.

Table 1. Combination factors ψ_0 for buildings (from prEN 1990 [23]).

Action	ψ_0
Imposed loads in buildings:	
Category A: domestic, residential areas	0.7
Category B: office areas	0.7
Category C: congregation areas	0.7
Category D: shopping areas	0.7
Category E: storage areas	1.0
Category F: traffic area	0.7
Category H: roofs accessible for normal maintenance	0.7
Wind actions on buildings	0.6

Table 2. Partial factors on actions for persistent and transient design situations and structural resistance verifications (from prEN 1990 [23]).

Action	γ_{G} or γ_{Q}
Permanent action G_{k}	1.35 (unfavourable) 1.00 (favourable)
Variable action Q_{k}	1.50 (unfavourable) 0.00 (favourable)

It is important to note that, for simplicity, the load factors adopted in the reliability calibrations for the development of the system-based direct design methodology were those prescribed in prEN 1990 [23]. Hence, the characteristic values of the loads and the

load factors to be adopted in the system-based direct design of structures are the same used in the traditional member-based *two-step* approach.

The combination of actions for the verifications of Serviceability Limit States (SLS) should be appropriate for the serviceability requirements and performance criteria under consideration. The characteristic combination of actions according to prEN 1990 [23] for SLS verifications is given in Eq. 3.

$$\sum F_{\mathrm{d}} = \sum_{i} G_{\mathrm{k,i}} + Q_{\mathrm{k},1} + \sum_{j>1} \psi_{0,\mathrm{j}} Q_{\mathrm{k,j}} \qquad \text{Eq. 3}$$

3. ULTIMATE LIMIT STATE CHECKS

3.1. INTRODUCTION

System-based direct design approaches have been developed in the Load and Resistance Factor Design (LRFD) framework and the Limit State philosophy familiar to most international structural engineers. Thus, these design recommendations assume that both the Ultimate Limit State (ULS) and Serviceability Limit State (SLS) verifications are satisfied, each of which uses specific load combinations.

This Section presents the Ultimate Limit State (ULS) verification process for system-based direct design approaches, and sets out the system partial safety factors $\gamma_{\mathrm{M,s}}$ calibrated for the direct design of cold-formed stainless steel portal frames in the NewGeneSS project.

3.2. ULS DESIGN CHECKS IN SYSTEM-BASED DIRECT APPROACHES

Current specifications for the design of steel structures are based on the Load and Resistance Factor Design (LRFD) and on the limit state criteria. The traditional design (verification) process follows two steps (that is why this design approach is also known as the *two-step* approach), in which the internal forces are first determined at each member and connection comprising the structure from a usually elastic analysis, and the resistance of each member is subsequently checked. For Ultimate Limit State (ULS) checks, the resistance of members and connections is verified using the provisions prescribed in the relevant structural specifications such as prEN 1993-1-4 [21] and prEN 1993-1-1 [24], generally assuming that the ultimate resistance of the structure is reached when the first member or connection reaches its ultimate limit state. In the traditional *two-step* design approach, design parameters are modelled by nominal or characteristic values and their random variations are accounted for through the use of partial safety or resistance factors.

Conversely, the design process and LRFD resistance check is very simple when system-based direct design approaches are considered, as given in Eq. 4,

$$R_{\mathrm{k}}/\gamma_{\mathrm{M,s}} = \sum \gamma_{\mathrm{i}}\, S_{\mathrm{k,i}} \qquad \text{Eq. 4}$$

where R_k is the characteristic resistance of the system, $S_{k,i}$ are the characteristic structural loads, γ_i are the corresponding load factors, and $\gamma_{M,s}$ denotes the safety factor of the system. In this direct system-based approach, the characteristic (or nominal) resistance of the system is derived from an advanced finite element model, which is further discussed in the following Chapters of this document.

Since the design loads are typically applied incrementally in advanced finite element analyses, the load scaling factor λ can be used as the governing parameter instead of the characteristic resistance R_k. In such cases, the resistance of the system at the state of incipient collapse is determined by the ultimate load scale factor λ_u and the LRFD equation shown in Eq. 4 simplifies to Eq. 5

$$\lambda_u \geq \gamma_{M,s} \qquad \text{Eq. 5}$$

Figure 2 illustrates a typical load scaling factor-deflection curve derived from an advanced finite element model for ULS checks in the system-based direct design approach and the definition of the ultimate load scale factor λ_u that determines the resistance of the system, which is further discussed in Section 10.3.

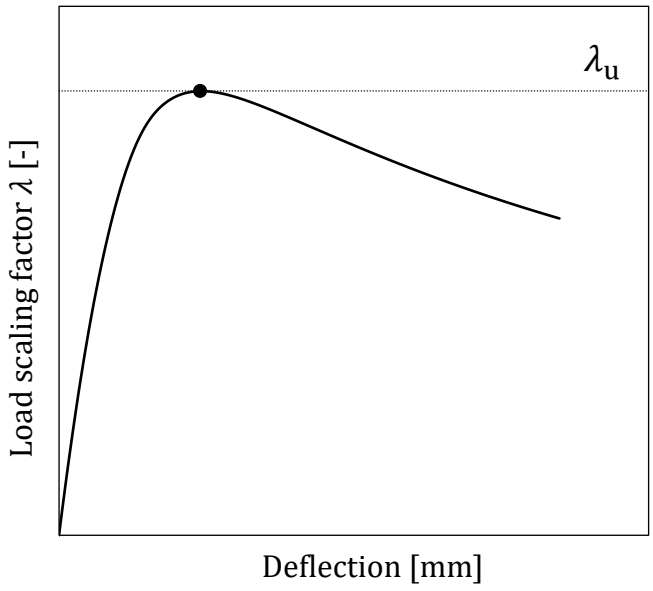

Figure 2. Typical load scaling factor-deflection curve for ULS checks in system-based direct design approaches.

3.3. SYSTEM FACTORS FOR THE DIRECT DESIGN OF STAINLESS STEEL FRAMES

Although some of the major international specifications for the design of steel structures already incorporate preliminary versions of system-based direct design approaches, the system partial safety factors $\gamma_{M,s}$ that need to be used when verifying structures as systems are not generally prescribed. Specifications generally require that designs carried out using system-based direct design approaches provide "a comparable or higher level of reliability" than that achieved for the traditional member-based provisions, but they do not provide guidance on how this may be guaranteed.

In order to calibrate suitable system partial safety factors $\gamma_{M,s}$ for the system-based direct design of steel and stainless steel structures under different loading conditions, robust reliability analyses have been carried out over the last decade for different types of materials and structure types. Table 3 reports the system partial safety factors $\gamma_{M,s}$ calibrated in [15,16] for their use in the system-based direct design of cold-formed stainless steel portal frames under different loading scenarios.

Table 3. System partial safety factors calibrated for stainless steel frames.

Loading scenario	System partial safety factor
Gravity loads	$\gamma_{M,s} = 1.15$
Dead and wind loads	$\gamma_{M,s} = 1.20$

System resistance factors calibrated for cold-formed stainless steel portal frames for the US-ASCE and Australian design frameworks can be also found in [15,16]. In addition, system factors for the direct design of other structure types (structural steel and cold-formed steel 2D and 3D frames, portal frames, storage rack frames and scaffolding systems) have also been calibrated for the US-ASCE and Australian design frameworks, and can be found in the literature [7-12].

4. SERVICEABILITY LIMIT STATE CHECKS

4.1. INTRODUCTION

Serviceability Limit States (SLS) are conditions at which the normal operation of structures is impacted or affected as a result of severe deformations of components, which can result in occupant discomfort, damages to machinery or services, and local damage. Although violations of Serviceability Limit States (SLS) do not generally result in safety issues, and hence they are not associated with partial safety or resistance factors, they may have significant economic consequences and they need to be carefully addressed in structural design. The most common serviceability non-compliances include excessive deflection of horizontal members or lateral displacement of structures, and vibrations.

While Serviceability Limit State checks should be addressed regardless of the approach chosen for the design of the structure, when system-based direct approaches are adopted for stainless steel structures serviceability considerations may become more relevant since the full exploitation of the capacity of sustaining large deformations before collapse generally leads to lighter structures and larger deformations. Combined with the nonlinear material response exhibited by stainless steel alloys even for low levels of strain, the adoption of system-based direct design approaches requires greater attention to serviceability limit states in such structures. This has been investigated in [17], where the influence of allowing larger deformations in the ultimate limit state design on serviceability considerations for stainless steel structures is assessed.

4.2. SLS DESIGN CHECKS IN SYSTEM-BASED DIRECT APPROACHES

The serviceability limit state criteria in steel structures generally include deflections and vibrations. As for the traditional design approach, the serviceability verifications for system-based direct design approaches require that the deflection of the system under the applied service loads Δ be lower than a certain allowable deflection limit δ_a, as indicated in Eq. 6.

$$\Delta \leq \delta_a \qquad \text{Eq. 6}$$

The deflection of the system Δ should be determined from a suitable structural analysis and the service loads that correspond to the relevant SLS load combination prescribed in prEN 1990 [23]. While elastic analyses are typically sufficient to determine Δ when the design of steel structures is based on the traditional *two-step* approach, it is necessary to perform fully nonlinear analyses using advanced finite element models for the system-based direct design approach. In the case of stainless steel structures, it is fundamental to account for the effect of the nonlinear material behaviour, which can be implicitly taken into account through the input of an accurate stress–strain relationship in the advanced FE models.

On the other hand, the allowable deflection limits δ_a are generally defined by the building authorities or the engineer, or are specified in the relevant structural codes or design manuals. The most usual deflection limits for steel frames correspond to vertical deflections under gravity loads and to lateral displacements under lateral (wind) loads, which are illustrated in Figure 3.

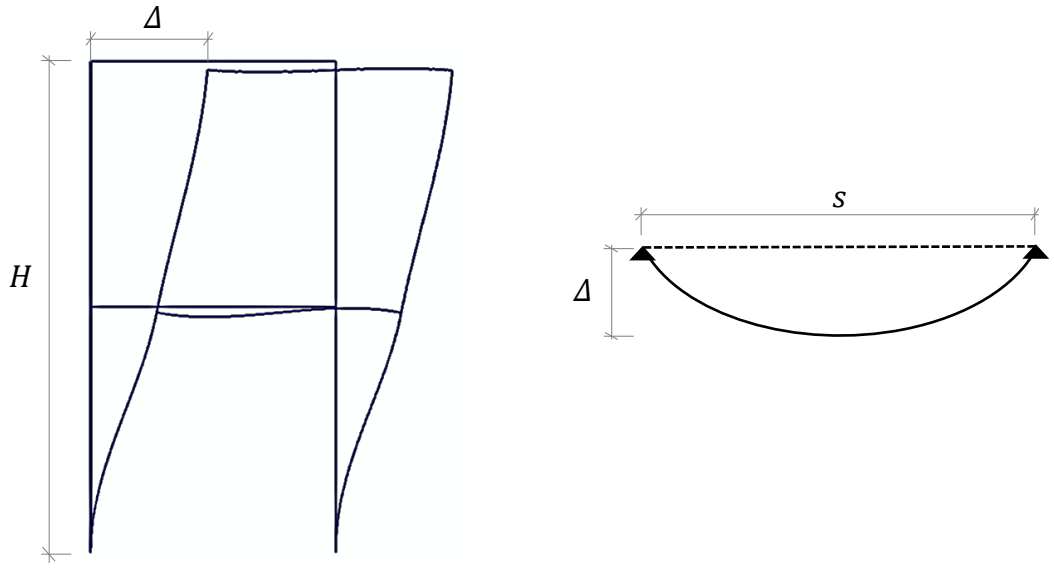

Figure 3. Definition of vertical deflections and lateral displacements for SLS checks.

Common limiting values for vertical deflections under gravity loads and to lateral displacements under lateral (wind) loads are reported in Table 4 and Table 5, respectively, where s is the frame span and H is the height of the frame.

Table 4. Allowable vertical deflection limits $\delta_{a,v}$ for steel structures.

Limit	Structure type	Loads	Source
$s/125$ $s/250$	Not accessible resilient roof Accessible resilient roof	Imposed load	[23]
$s/240$	Roof members	Imposed load	[25]
$s/300$	Roof members	Long-term gravity loads	[26]
$s/200$	Roofs in general	Total loads	[27]
$s/250$	Roofs in general	Imposed load	[27]
$s/360$ $s/500$	Frames with pitch angle > 3º Frames with pitch angle < 3º	Dead load	[28]
$s/240$	–	Imposed load	[28]
$s/150$	–	Wind load	[28]
$s/250$	–	–	[29]

Table 5. Allowable lateral displacement limits $\delta_{a,h}$ for steel structures.

Limit	Structure type	Loads	Source
$H/300$	–	Wind load	[6,9]
$H/400$	Single storey buildings	–	[23]
$H/600$-$H/400$	–	Wind load	[25]
$H/500$	Side sway in columns	Wind load	[26]
$H/400$	–	Wind load	[30]
$H/150$	Portal frames without gantry crane	Total loads	[27]
$H/150$	Portal frames without fragile elements	Total loads	[31]
$H/300$	Single-storey buildings with horizontal roofs without fragile elements	Total loads	[31]
$H/150$	Portal frame with metal cladding	Service wind	[28]

5. DEVELOPMENT OF NOMINAL ADVANCED ANALYSIS MODELS

The design of stainless steel frames using system-based direct design approaches requires the development of sophisticated finite element models capable of reproducing the response and resistance of structural systems with great accuracy. While in the traditional *two-step* design approach the consideration of some initial imperfections and geometric nonlinearities (second-order analyses) is generally sufficient in the structural analysis step, system-based direct design approaches require the consideration of all the relevant features that can affect the behaviour of systems. This generally requires the use of advanced finite element software and suitable guidance on how to build the nominal models from which the characteristic (or nominal) system resistances can be retrieved. The features that need to be implemented into the nominal advanced models include initial geometric imperfections and a nonlinear material response, among others, and are prescribed in the specifications relevant to the design framework and structure type considered, which will indicate the nominal values and shapes of these features.

In general, nominal advanced models should account for the following effects:

- Geometric nonlinearities
- Material nonlinearities: actual (nonlinear) material response
- Initial geometric imperfections at global, member and local levels
- Residual stresses
- Actual behaviour of connections

This document presents and discusses, in the following chapters, each of these features with a special emphasis on the Eurocode design framework and cold-formed stainless steel structures. Aspects related to the actual (nonlinear) material response of stainless steel alloys are presented in Chapter 6, while Chapter 7 discusses the different types of initial geometric imperfections. Residual stresses are covered in Chapter 8 and the behaviour of connections in Chapter 9. Finally, Chapter 10 describes the different types of structural analysis and how the characteristic (nominal) system resistances can be obtained from advanced finite element models.

6. MATERIAL BEHAVIOUR

The stress–strain relationship of stainless steel alloys typically used in construction or structural applications is pronouncedly nonlinear and ductile, with considerable strain hardening. Since system-based direct design approaches fully exploit the benefits of this ductility and strain hardening, more efficient designs than those obtained using the traditional design approaches can be achieved. For this reason, it is fundamental to use advanced finite element software capable of accounting for this nonlinear behaviour in the analysis and to have material models that describe the actual stress–strain relationship accurately.

For a correct definition of the material behaviour, two aspects are necessary: a material model that accurately reproduces the actual stress-strain relationship and suitable values of the material parameters involved in the model. This Chapter presents the constitutive model developed for stainless steel alloys, introduces the values for the basic nominal material parameters and provides guidance on additional considerations such as the enhanced material properties for cold-formed sections and the adoption of particular material curves for advanced simulation software.

6.1. MATERIAL MODEL FOR STRESS–STRAIN RELATIONSHIPS

The nonlinear stress–strain ($\sigma - \varepsilon$) behaviour exhibited by stainless steel alloys can be accurately described by the two-stage Ramberg-Osgood material model proposed in [32], which is given in Eq. 7 and Eq. 8 and uses different material parameters in its definition. This material model refers to the engineering stress–strain relationship, and it has been adopted in the European specifications prEN 1993-1-14 *Design assisted by finite element analysis* [4] and prEN 1993-1-4 *Supplementary Rules for Stainless Steels* [21].

$$\varepsilon = \frac{\sigma}{E} + 0.002\left(\frac{\sigma}{f_{\mathrm{y}}}\right)^{n} \qquad \text{for } \sigma \le f_{\mathrm{y}} \qquad \text{Eq. 7}$$

$$\varepsilon = \frac{\sigma - f_{\mathrm{y}}}{E_{0.2}} + \left(\varepsilon_{\mathrm{u}} - \varepsilon_{0.2} - \frac{f_{\mathrm{u}} - f_{\mathrm{y}}}{E_{0.2}}\right)\left(\frac{\sigma - f_{\mathrm{y}}}{f_{\mathrm{u}} - f_{\mathrm{y}}}\right)^{m} + \varepsilon_{0.2} \qquad \text{for } f_{\mathrm{y}} \le \sigma \le f_{\mathrm{u}} \qquad \text{Eq. 8}$$

The material parameters necessary to describe the stress–strain ($\sigma - \varepsilon$) relationship are the Young's modulus E, the yield stress f_{y}, the first strain hardening exponent n, the

ultimate tensile strength f_u, the ultimate strain ε_u and the second strain hardening exponent m. In Eq. 8, $\varepsilon_{0.2}$ is the total deformation at the yield stress $\varepsilon_{0.2} = 0.002 + f_y/E$ and $E_{0.2}$ is the corresponding tangent modulus, which can be estimated from Eq. 9.

$$E_{0.2} = \frac{E}{1 + 0.002n\,E/f_y} \qquad \text{Eq. 9}$$

The typical two-stage Ramberg-Osgood stress–strain curve is shown in Figure 4, where the key material parameters are also defined.

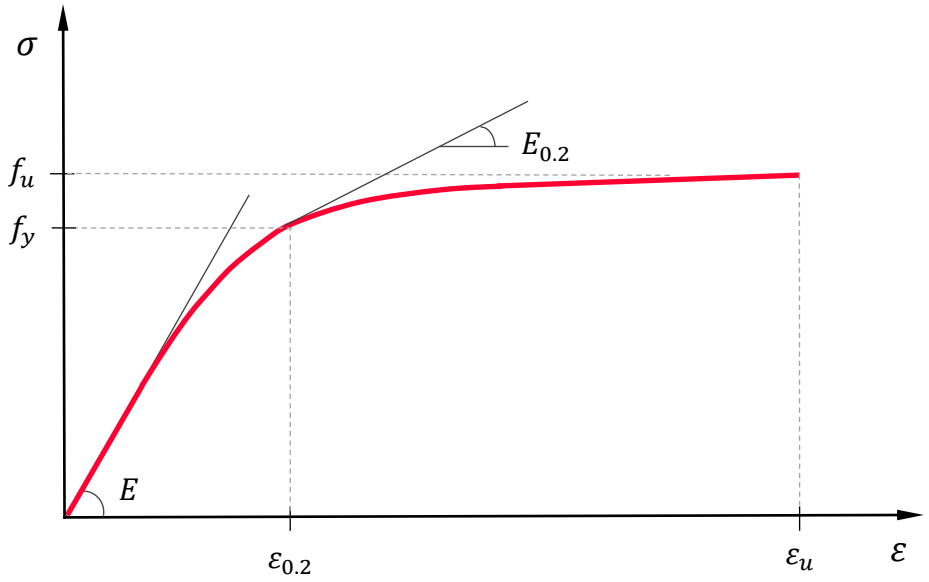

Figure 4. Typical two-stage Ramberg-Osgood stress–strain curve with definitions of key material parameters.

The values of the basic material parameters (i.e., E, f_y and f_u) are generally prescribed in structural or material standards, including prEN 1993-1-4 [21], or product specifications. Expressions for predicting the remaining material properties from the basic parameters are also available in the different standards and design manuals, including prEN 1993-1-14 [4] and the Design Manual for Structural Stainless Steel [33]. The ultimate strain ε_u can be determined from Eq. 10 or Eq. 11 for austenitic or duplex, and ferritic grades, respectively, while the first and second strain hardening parameters n and m can be estimated from Eq. 12 and Eq. 13, where $\sigma_{0.05}$ is the 0.05% proof stress.

$$\varepsilon_u = 1 - \frac{f_y}{f_u} \quad \text{for austenitic and duplex grades} \qquad \text{Eq. 10}$$

$$\varepsilon_{\mathrm{u}} = 0.6\left(1 - \frac{f_{\mathrm{y}}}{f_{\mathrm{u}}}\right) \quad \text{for ferritic grades} \qquad \text{Eq. 11}$$

$$n = \frac{\ln(4)}{\ln\left(\frac{f_{\mathrm{y}}}{\sigma_{0.05}}\right)} \qquad \text{Eq. 12}$$

$$m = 1 + 2.8\frac{f_{\mathrm{y}}}{f_{\mathrm{u}}} \qquad \text{Eq. 13}$$

Alternatively, the recommended values for the first strain hardening parameter n to be adopted when $\sigma_{0.05}$ is unknown, as per prEN 1993-1-4 [21], are reported in Table 6.

Table 6. Recommended values of n for different stainless steel families [21,32].

Stainless steel family	Recommended value of n
Austenitic	7
Duplex	8
Ferritic	14

The minimum longitudinal nominal basic material properties (i.e., the Young's modulus E, the yield stress f_{y} and the ultimate tensile strength f_{u}) for the most common stainless steel grades, as prescribed in EN 10088-4 [34], are reported in Table 7. It should be noted that prEN 1993-1-4 [21] recommends a single value of the Young's modulus of 200,000 N/mm^2 for all stainless steel families, while in EN 10088-4 [34] ferritic alloys are prescribed a slightly higher value. Figure 5 shows the stress–strain relationships for typical duplex (1.4462), ferritic (1.4003) and austenitic (1.4301) grades.

Table 7. Nominal material properties for common stainless steel grades from [34].

Stainless steel family	Stainless steel grade	E [N/mm^2]	f_{y} [N/mm^2]	f_{u} [N/mm^2]
Austenitic	1.4301	200,000	230	550
	1.4401	200,000	240	530
Duplex	1.4462	200,000	500	700
	1.4162	200,000	530	700
Ferritic	1.4003	220,000	280	450
	1.4016	220,000	260	450

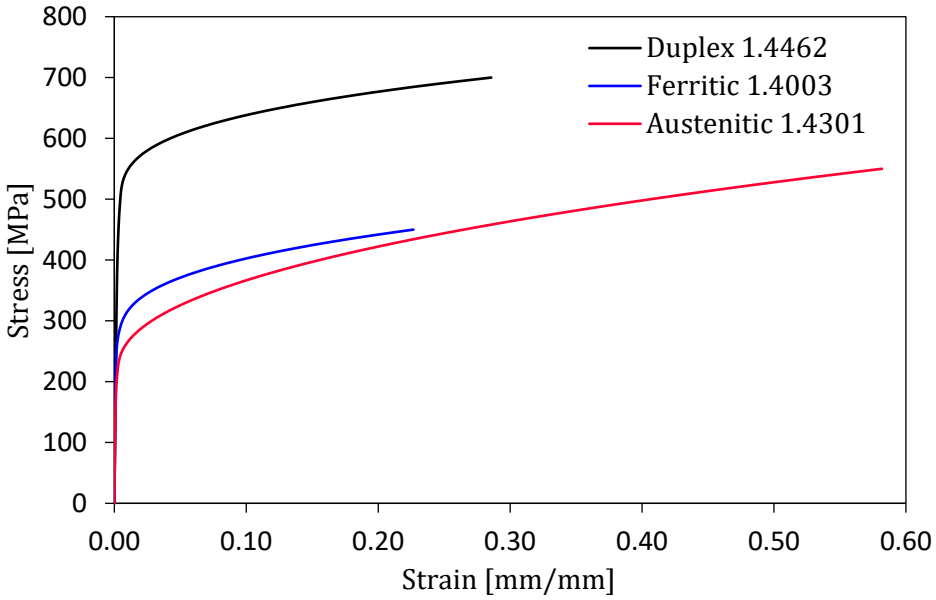

Figure 5. Nominal stress–strain relationships for typical duplex, ferritic and austenitic stainless steel grades.

However, it is important to note that some commercial finite element software require the input of material properties based on plastic strains instead of on the total strains, starting at the proportionality limit of the material (stress beyond which the material does not behave elastically. For these situations, the plastic strain corresponding to each level of stress should be calculated using Eq. 14 and the proportional limit can be assumed as the stress at which the plastic strain is equal to $\varepsilon_{\mathrm{pl}} = 1 \cdot 10^{-5}$ (approximately the $\sigma_{0.05}$ proof stress).

$$\varepsilon_{\mathrm{pl}} = \varepsilon - \frac{\sigma}{E} \qquad \text{Eq. 14}$$

6.2. COLD-FORMED STAINLESS STEEL

Cold-formed stainless steel members, especially tubular members, constitute one of the most common stainless steel product types. They allow combining the high strength-to-weight ratios exhibited by cold-formed sections with the excellent corrosion resistance of stainless steels, resulting in very versatile products. Nevertheless, the cold forming process significantly affects the material characteristics of the sheet material, enhancing the strength and reducing the ductility, and these modifications need to be taken into account for an accurate definition of the stress–strain relationship in advanced FE

models. For this, the models predicting the reduction in ductility and the enhancement in strength enhancement available in design standards can be used.

Provisions to calculate the enhanced material properties of cold-formed stainless steel products can be found in prEN 1993-1-4 [21] or the Design Manual [33], and are based on the work carried out in [35]. These provisions provide guidance on the estimation of the average enhanced yield stress f_{ya} of cold-formed cross-sections and although only the expressions corresponding to cold-formed rectangular hollow sections are reproduced in this document, additional predictive equations can be found in [21,33] for other cross-section shapes.

The average enhanced yield stress f_{ya} can be estimated as a weighted average yield stress considering the enhanced yield stresses of the corner f_{yc} and flat f_{yf} regions of the cross-section, as shown in Eq. 15, where A is the gross area of the cross-section and A_c is the total corner cross-sectional area, which for cold-rolled rectangular and square hollow sections can be determined from Eq. 16, being n_c the number of 90° corners and r the internal bend radius, which may be taken as t if not known, as recommended in [14].

$$f_{ya} = \frac{A_c f_{yc} + (A - A_c) f_{yf}}{A} \qquad \text{Eq. 15}$$

$$A_c = \left(n_c \pi \frac{t}{4}\right)(2r + t) + 4 n_c t^2 \qquad \text{Eq. 16}$$

The enhanced yield stress of the corner f_{yc} and flat f_{yf} regions can be calculated from Eq. 17 and Eq. 18, respectively, where ε_c and ε_f are the strains induced in the corner and flat areas during section forming, and n_p is given by Eq. 19.

$$f_{yc} = 0.85 f_y \left(\frac{\varepsilon_c}{\varepsilon_{0.2}} + 1\right)^{n_p} \quad \text{but} \quad f_y \le f_{yc} \le f_u \qquad \text{Eq. 17}$$

$$f_{yf} = 0.85 f_y \left(\frac{\varepsilon_f}{\varepsilon_{0.2}} + 1\right)^{n_p} \quad \text{but} \quad f_y \le f_{yt} \le f_u \qquad \text{Eq. 18}$$

$$n_p = \frac{\ln(f_y / f_u)}{\ln(\varepsilon_{0.2} / \varepsilon_u)} \qquad \text{Eq. 19}$$

The strains induced in the corner ε_c and flat ε_f regions during section forming can be estimated from Eq. 20 and Eq. 21,

$$\varepsilon_c = \frac{t}{2(2r+t)} \quad \text{Eq. 20}$$

$$\varepsilon_f = \frac{t}{900} + \frac{\pi t}{2(b+h-2t)} \quad \text{Eq. 21}$$

Finally, the average tensile strength f_{ua} can be calculated from the relationships given in Eq. 22 and Eq. 23, respectively, for austenitic or duplex, and ferritic grades.

$$f_{ua} = \frac{f_{ya}}{0.20 + 185\frac{f_{ya}}{E}} \quad \text{for austenitic and duplex grades} \quad \text{Eq. 22}$$

$$f_{ua} = \frac{f_{ya}}{0.46 + 145\frac{f_{ya}}{E}} \quad \text{for ferritic grades} \quad \text{Eq. 23}$$

6.3. TRUE STRESS–STRAIN RELATIONSHIPS

The material model described in Section 6.1 concerns engineering stresses and strains. However, it is necessary to convert these stresses and strains into true stresses and strains when the advanced finite element models utilize solid element models or shell elements with thickness reduction effect (i.e., cases in which material contractions are involved). The true stress–true strain ($\sigma_{true} - \varepsilon_{true}$) relationship can be determined from the engineering curve defined in Section 6.1 adopting Eq. 24 and Eq. 25.

$$\sigma_{true} = \sigma \cdot (1 + \varepsilon) \quad \text{Eq. 24}$$

$$\varepsilon_{true} = \ln(1 + \varepsilon) \quad \text{Eq. 25}$$

Figure 6 presents the comparison of the engineering and true stress–strain relationships for the nominal 1.4301 austenitic stainless steel grade.

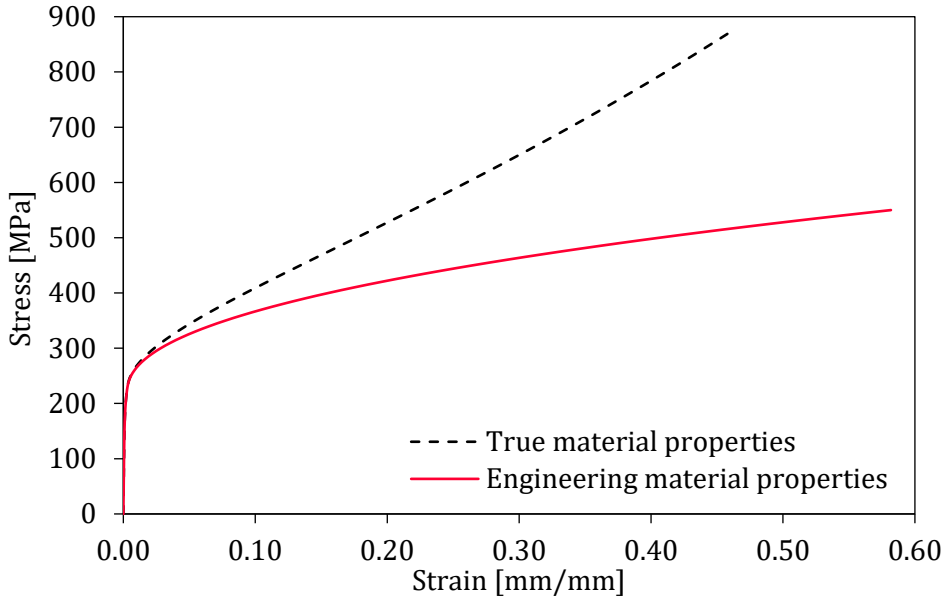

Figure 6. Comparison of the nominal engineering and true stress–strain relationships for the austenitic stainless steel grade 1.4301.

When the software used to build the nominal advanced models requires the input of plastic strains in the definition of the material properties, these can be determined from Eq. 14 but using the true stress–strain relationship instead of the engineering material curve.

7. INITIAL GEOMETRIC IMPERFECTIONS

Initial geometric imperfections are a fundamental feature of steel and stainless steel structures that may have a significant influence on the response and resistance of steel systems since they introduce additional load eccentricities and increase second-order effects, causing the premature failure of the structure. Initial geometric imperfections occur inevitably despite the strict manufacturing and installation tolerance requirements, and thus they need to be explicitly introduced in the advanced finite element models for an accurate determination of the system resistance.

Initial geometric imperfections relevant to stainless steel frames primarily include out-of-plumb frame imperfections and out-of-straightness member imperfections, although cross-section imperfections should also be considered for locally unstable structures. For each imperfection type, structural design specification such as prEN 1993-1-4 [21] and prEN 1993-1-14 [4], which refer to prEN 1993-1-1 [24] for some types of imperfections, include clauses that define the shapes and amplitudes of such imperfections. Specifications also prescribe how the different imperfection types should be input into the advanced FE models, and how the different imperfections should be combined. This Chapter provides a thorough overview of initial geometric imperfections and provides guidance on how to model them when carrying out a system-based direct design of stainless steel frames.

7.1. SHAPE AND AMPLITUDE OF INITIAL GEOMETRIC IMPERFECTIONS

This Section details the shape and amplitude of the different types of initial geometric imperfections that should be introduced in advanced finite element models for an accurate prediction of the resistance of stainless steel frames. Recommendations are given, based on European structural design provisions, for the definition of global sway imperfections, member imperfections and local imperfections.

7.1.1. Initial global sway imperfections

Initial global imperfections are deviations of the overall structure from the perfect geometry, the most representative of which are sway-shaped initial imperfections. The sway imperfection is an out-of-plumbness, with all columns leaning in the same direction, defined by a drift angle ϕ, as shown in Figure 7. Owing to the importance of these

imperfections and the influence they may have in the resistance and stiffness of systems, they need to be incorporated in the advanced finite element models. Although the maximum column inclination deviation of portal frames according to the erection tolerances given in EN 1090-2 [36] is $\phi = \pm 1/500$, and the measurements on actual steel structures indicate mean drift angles of about $\phi = \pm 1/770$, different and more conservative values of the ϕ-angle are generally adopted in design.

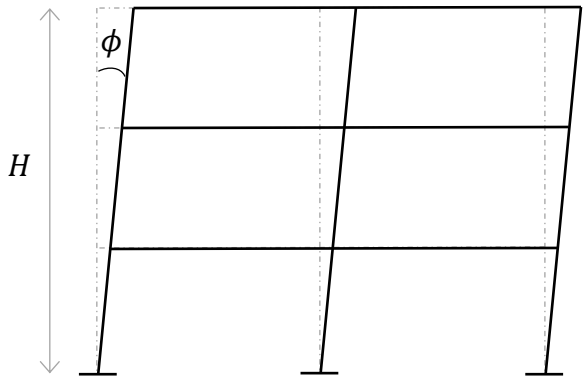

Figure 7. Initial sway imperfections.

According to §7.3.2 of prEN 1993-1-1 [24], the design (nominal) out-of-plumb angle ϕ is calculated from Eq. 26, where ϕ_0 is the basic value of the initial sway imperfection. This parameter adopts a value of $\phi_0 = 1/400$ when the resistance checks are based on elastic verifications, and $\phi_0 = 1/200$ when the checks are based on plastic verifications. Considering that advanced simulations will be typically based on plastic analyses, the basic value of the initial sway imperfection will generally be $\phi_0 = 1/200$ in the context of system-based direct design approaches.

$$\phi = \phi_0 \alpha_{\mathrm{H}} \alpha_{\mathrm{m}} \qquad \text{Eq. 26}$$

The basic value ϕ_0 is multiplied by the reduction factors for the height α_{H} and for the number of columns in a row α_{m}, which are given by Eq. 27 and Eq. 28, respectively, in which H is the height of the structure in metres and m is the number of columns in a row, including only those carrying a vertical load N_{Ed} not less than 50% of the average value of all the columns in the vertical plane considered.

$$\alpha_{\mathrm{H}} = 2/\sqrt{H} \qquad \text{Eq. 27}$$

$$\alpha_{\mathrm{m}} = \sqrt{0.5\left(1 + \frac{1}{m}\right)} \qquad \text{Eq. 28}$$

The initial sway imperfection should be applied in all relevant horizontal directions but considering only one direction at a time. Moreover, sway imperfections in building frames may be disregarded when $H_{\mathrm{Ed}} \geq 0.15 F_{\mathrm{Ed}}$, where H_{Ed} is the total design horizontal load and F_{Ed} is the total design vertical load.

7.1.2. Initial member bow imperfections

Initial member imperfections are bow-shaped deviations from the perfect member geometry in which cross-sections are displaced or rotated as whole, and are generally associated with member buckling shapes, as shown in Figure 8(a). These initial member imperfections have a considerable effect on member capacity as they increase second-order effects and can cause premature failure. As for global sway imperfections, design (nominal) values of the member bow imperfections significantly higher than the average measured imperfections need to be considered in design.

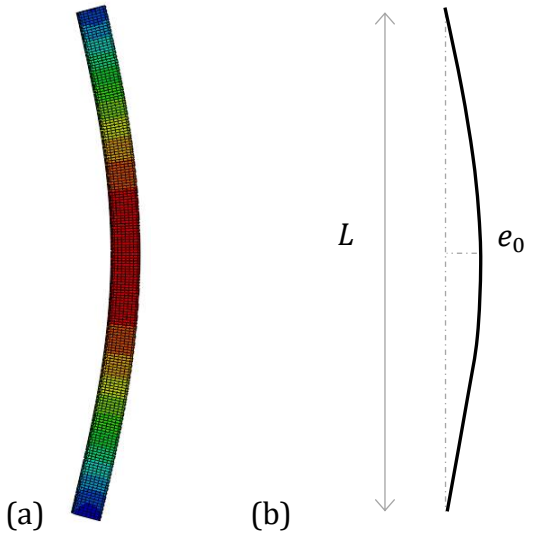

Figure 8. Initial member bow imperfections.

For member bow imperfections, prEN 1993-1-14 [4] recommends an imperfection amplitude e_0 equal to 80% of the geometric manufacturing tolerances given in EN 1090-2 [36], with a minimum value of $e_0 = L/1000$, and a half-sinusoidal shape along the member length L, as shown in Figure 8(b). In-plane and out-of-plane member bow imperfections should be introduced (when physically relevant), and the two possible directions should be considered for each imperfection.

7.1.3. Initial local imperfections

Initial local cross-section imperfections are defined as deviations of the different plate elements comprising the cross-section from the perfect geometry, and include distortional-shaped and local-shaped modes. For cold-formed hollow sections (SHS, RHS and CHS) the latter are more relevant, since the transverse stiffness of hollow sections is remarkably high, whereas for open sections (including I-sections and channels) both types can be important.

Currently, prEN 1993-1-14 [4] only provides guidance on the magnitudes of local imperfections for outstand elements and distortional buckling in cold-formed sections, but not for the cold-formed hollow sections covered by this document. Provisionally, the Dawson and Walker model can be assumed to estimate the amplitude of the local imperfection w_0, as given in Eq. 29, which was calibrated for stainless steel hollow sections by [37] adopting a $\gamma = 0.023$ coefficient.

$$w_0 = \gamma \frac{f_y}{\sigma_{cr}} t \qquad \text{Eq. 29}$$

Local imperfections should be introduced when the members that comprise the system under investigation are susceptible of failure modes that involve local failure, cases in which shell-type finite element models should be adopted. In those cases, the shape of the local imperfections (similar to that shown in Figure 9) should be determined from a prior eigenvalue analysis.

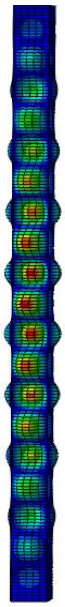

Figure 9. Initial local imperfections on tubular sections.

7.2. MODELLING INITIAL GEOMETRIC IMPERFECTIONS

Once the shape and amplitude of the different types of initial geometric imperfections are determined, different alternatives exist for modelling and inputting these imperfections in the advanced models depending on the commercial finite element software available. The most common approaches to consider the effects of initial geometric imperfections in advanced analysis include: 1) the modelling of imperfections by directly offsetting the coordinates of the nodes, 2) the reduction of member stiffness, 3) the adoption of notional horizontal forces, and 4) the superposition of scaled elastic buckling modes.

While the direct offset of the node coordinates is sometimes possible for some particular structural analysis software, it is generally not practical for everyday engineering practice. In this regard, the stiffness reduction method is an interesting approach since it does not require an explicit modelling of the imperfections. However, and although several stiffness-reduction factors have been proposed in the literature to account for the effect of initial geometric imperfections, they generally also account for additional considerations such as residual stresses or the effect of plasticity, being impossible to identify the part of the reduction factor that corresponds to member or local initial geometric imperfections only.

Alternatively, the notional horizontal force method has been widely adopted in different structural standards, including prEN 1993-1-1 [24], for its simplicity and because it allows modelling structures in their theoretically perfect configuration and taking into account the effect of initial geometric imperfections by introducing a set of notional horizontal forces. While the introduction of sway and member imperfections through this method is correct for the traditional *two-step* design approach, only global sway imperfections can be input via notional forces for the design and verification of steel structures using system-based direct design approaches. In such cases, the effects of sway imperfection may be replaced by systems of notional (equivalent) horizontal forces, introduced at each floor and at the roof level, as shown in Figure 10. Note that, in order to introduce a self-equilibrated system of equivalent forces, the corresponding loads should be introduced at the base of the frames.

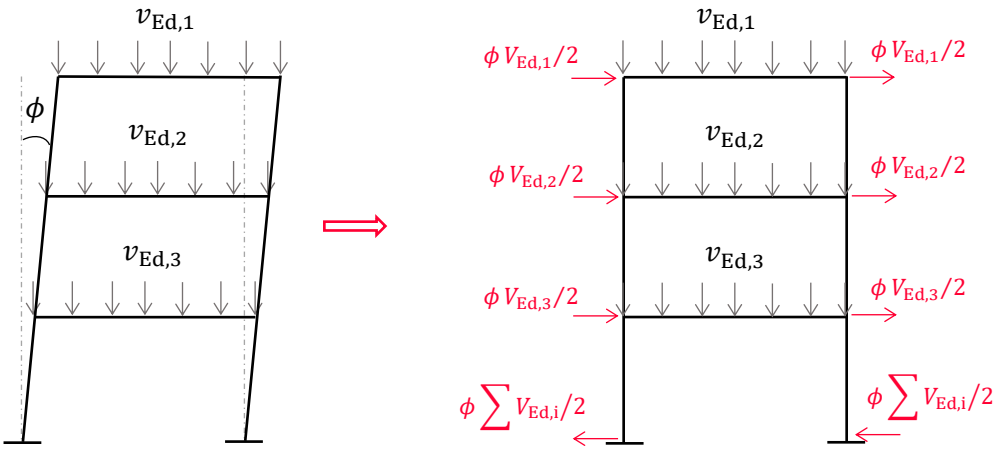

Figure 10. Replacement of initial sway imperfection by equivalent horizontal forces.

Another option to model initial geometric imperfections prescribed in §7.3.6 of prEN 1993-1-1 [24] is to use scaled elastic buckling modes, assuming that the first eigenmode represents the most critical imperfection shape. Although this is the approach typically adopted when the traditional member-based *two-step* design approach is considered, the significant plastic deformations and load redistributions that occur in advanced analysis can result in failure modes involving parts of the structure deficiently represented by the first buckling mode. To ensure that imperfections are introduced in virtually all members, it is recommended to adopt the approach developed in [38] and to include additional higher order eigenmodes when inputting initial geometric imperfections. This procedure is based on the superposition of six scaled buckling modes, with the imperfection amplitudes of each mode A_i being determined from Eq. 30,

$$A_i = \begin{cases} P_i \cdot F \cdot H & \text{for sway modes} \\ P_i \cdot F \cdot L & \text{for non-sway modes} \end{cases} \qquad \text{Eq. 30}$$

where P_i is the normalized participation factor for the i^{th} buckling mode, F is the amplitude factor (equal to F=0.003), and H and L are the frame height and member length, respectively. The participation factors P_i, summarized in Table 8 for unbraced and braced frames, were calibrated for a range of low-to-mid-rise frames under gravity loads. It should be noted that even if the P_i and F factors were determined from actual initial imperfection measurements on steel frames, it is believed that these imperfection amplitudes represent an upper bound for stainless steel frames and can be also adopted for the design of stainless steel frames, since workshops for stainless steel structures are

generally more specialized and therefore final structures will typically present imperfections with lower amplitudes and levels of uncertainty.

Table 8. Participation factors to model initial geometric imperfections in frames.

Type of frame	P_1	P_2	P_3	P_4	P_5	P_6
Unbraced	0.40	0.10	0.15	0.15	0.10	0.10
Braced	0.20	0.20	0.15	0.15	0.15	0.15

7.3. COMBINATION OF INITIAL GEOMETRIC IMPERFECTIONS

Once the relevant initial geometric imperfection types and the corresponding amplitudes and shapes are defined and input into the advanced finite element models, it is necessary to combine the different imperfections and possible directions using the combination rules prescribed in specifications. In the Eurocode framework, prEN 1993-1-14 [4] provides guidance on how to combine initial geometric imperfections in section §5.5, which indicates that the different types of imperfections should be added linearly considering the imperfection directions resulting in the most critical combination of imperfection directions, and that the nominal resistance of the structure should be adopted as the smallest resistance value. When the relevant directions are not evident, several imperfection combinations with different directions should be investigated. This is generally not practical, since the number of possible imperfection combinations is significant even for relatively simple frames.

Recent studies [39] have shown that the influence of the combination of different imperfection directions on the resistance of common steel and stainless steel sway frames is small, since the variability of the ultimate loads for all the different imperfection direction combinations was found to be low. The study also demonstrated that the adoption of a linear combination of six buckling modes, following the approach developed in [38] and described in Section 7.2, with an arbitrary combination of the different modes (e.g., considering positive amplitudes for all six modes) is a simple yet congruous approach for modelling and combining initial geometric imperfections, since it provides nominal resistances close to the minimum frame resistance without requiring additional combinations to be investigated. However, it should be noted that the extension of these conclusions regarding imperfection type and direction combinations to non-sway frames is yet to be assessed.

8. RESIDUAL STRESSES

Residual stresses are stresses that exist in structural sections in their unloaded state, primarily generated during the fabrication processes, and which are particularly relevant in systems prone to instability failure modes as they can cause premature yielding and buckling, thus reducing their resistance. Residual stresses are caused either by the differential cooling of different parts of the cross-section (in hot-rolled and welded sections), in which membrane residual stresses govern, or by non-uniform plastic deformations (in cold-formed sections), in which bending residual stresses are more relevant. In addition to the fabrication process, the material and thermal properties of the alloy have a strong influence on the final residual stress pattern present in the members, and thus the residual stresses are different in equivalent stainless steel and structural steel sections, requiring the development of different and independent residual stress models.

According to prEN 1993-1-14 [4], residual stresses should be represented by initial strains or stresses in the finite element models, giving an equilibrium stress state without application of external loads. Moreover, the combination rules for residual stresses and initial geometric imperfections are given in §5.5 of prEN 1993-1-14 [4], which states that all initial geometric imperfections and residual stresses should be applied in the finite element model at the same time, using their nominal values without requiring specific combination rules.

This Chapter presents the residual stress models for the most commonly used stainless steel sections and provides guidance on how residual stresses may be modelled in advanced finite element models.

8.1. RESIDUAL STRESS MODELS FOR STAINLESS STEEL SECTIONS

Although prEN 1993-1-14 [4] prescribes suitable residual stress models for a range of materials and cross-section types in section §5.4.3, in the case of stainless steel cross-sections only models corresponding to welded stainless steel sections (i.e., welded I-sections and box sections) are included. Nevertheless, it is possible to use the models available in the literature when there is lack of specific guidance in specifications.

Figure 11 presents the residual stress model for welded stainless steel I-sections prescribed in prEN 1993-1-14 [4], which adopts slightly different distributions for different stainless steel families and welding types by using different values of the defining parameters, as reported in Table 9.

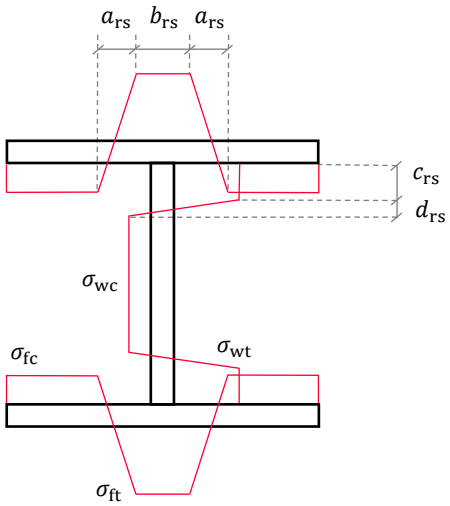

Figure 11. Residual stress model for welded stainless steel I-sections (adapted from [4]).

Table 9. Parameters for the residual stress model for welded stainless-steel I-sections.

Material type	Fabrication	$\sigma_{ft} = \sigma_{wt}$	$\sigma_{fc} = \sigma_{wc}$	a_{rs}	b_{rs}	c_{rs}	d_{rs}
Austenitic	Welded	$0.8f_y$	From equilibrium	$0.225b_f$	$0.05b_f$	$0.025h_w$	$0.225h_w$
Duplex, Ferritic		$0.6f_y$					
Austenitic, Duplex, Ferritic	Laser welded	$0.5f_y$	From equilibrium	$0.1b_f$	$0.075b$	$0.0375h_w$	$0.1h_w$

Alternatively, and despite being one of the most commonly adopted stainless steel product types, the current version of the prEN 1993-1-14 [4] specification does not include a residual stress model for cold-formed stainless steel SHS and RHS sections. Under such conditions, the model available in the literature and proposed in [40] can be adopted for these sections, which is shown in Figure 12. This model neglects membrane residual stresses, as they are not particularly high for these types of cross-sections, and defines bending residual stresses with magnitudes equal to $0.63f_y$ and $0.37f_y$ for the flat and corner regions of the cross-section, respectively. The model also assumes a

rectangular-block distribution through the thickness, with tensile bending residual stresses at the outer surface of the sections.

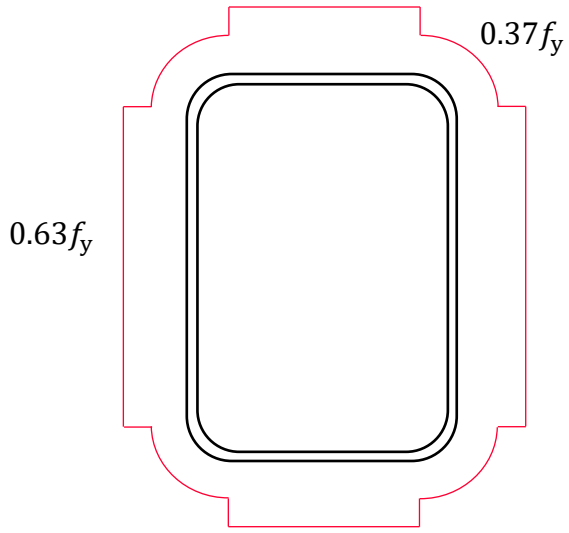

Figure 12. Residual stress model for cold-formed stainless steel SHS and RHS (adapted from [40]).

Additional suitable residual stress models for other types of stainless steel sections and fabrication processes may be found in the literature.

8.2. METHODS TO MODEL AND INPUT RESIDUAL STRESSES

Depending on the features of the software used to build the advanced finite element model, different alternatives exist for the consideration or input of residual stresses:

- model the state of initial stresses directly,
- use auxiliary user subroutines,
- modify the stress–strain relationship to account for residual stresses implicitly,
- use a stress–strain relationship obtained from tensile coupon tests that account for residual stresses implicitly, or
- consider a higher initial geometric imperfection in members to account for residual stresses also.

The choice of the final method adopted will typically depend on the information available to the designer and the capabilities of the software used for the analysis. Some analysis software incorporate pre-defined residual stress models for typical steel product types, which can be applied directly or adapted to fit existing models to different material types. In other cases, it is necessary to use auxiliary user subroutines, such as the SIGINI

subroutine in ABAQUS [41], to introduce the initial strains or stresses in the finite element models.

An alternative approach is to adopt a modified stress–strain diagram to account for residual stresses implicitly. On the one hand, in the case of cold-formed members it is possible to assume that the residual stresses are implicitly included in the stress–strain curves obtained from tensile coupon tests carried out on coupons that are cut from specimens. It is generally accepted that bending residual stresses release when the coupons extracted from cold-formed tubes curve longitudinally, which are re-introduced into the coupons when they return to their original straight shape as a result of the gripping and loading process at the tensile testing machine [42]. On the other hand, when the material behaviour is determined from the two-stage model provided in Chapter 6, the engineering stress–strain diagram can be modified to account for the effect of residual stresses following the methodologies developed in [43,44].

Finally, an additional simple alternative to input residual stresses in advanced finite element models is to adopt higher equivalent initial member imperfections e_0, similar to those described in Section 7.1.2, that account for the combined effect of out-of-straightness imperfections and residual stresses, as proposed in [45].

9. CONNECTIONS

9.1. MODELLING CONNECTION BEHAVIOUR IN ADVANCED ANALYSIS

According to EN 1993-1-8 [46], steel joints can be classified as rigid, semi-rigid and pinned connections depending on their stiffness, or as full-strength, partial-strength and pinned connections depending on their strength relative to the connected members. The type and behaviour of connections can have a remarkable effect on the response of steel structures, since internal forces and deflections will typically depend on the stiffness and resistance of the joints, and thus it is fundamental to account for this behaviour in the analysis by including it in the advanced finite element models.

The effect of the connection behaviour (stiffness and resistance) on the structural performance of stainless steel systems can be accounted for by modelling the moment–rotation response of the joint. The moment–rotation curve of steel connections can be reasonably represented by a bi-linear model defined through two stiffness parameters K_1, K_2 and two moment capacities M_1 and M_2, as shown in Figure 13. The nominal values of each parameter can be (i) chosen in accordance with the design requirements (and subsequently design connections that show this behaviour), or (ii) determined from the relevant standards using methods such as the component method in EN 1993-1-8 [46] or by means of specific software for the designed connections.

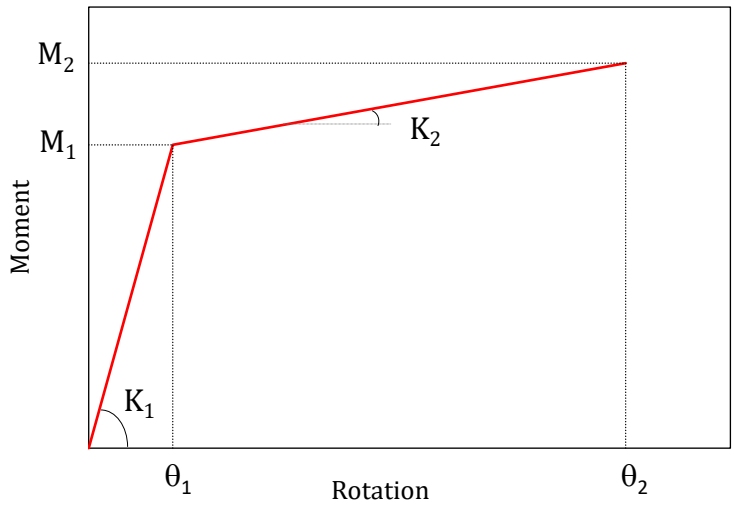

Figure 13. Typical moment–rotation model for connection behaviour.

9.2. RESISTANCE CHECKS IN CONNECTIONS

While the effect of connection behaviour on the response of stainless steel structures can be considered by modelling the moment–rotation diagrams characterizing the different joints, additional considerations are required to actually verify the resistance of the different connections. It is important to note that all research efforts made to date in the development of recommendations for the system-based direct design of steel and stainless steel structures have assumed that joints possess sufficient resistance and ductility for the ultimate limit states of the structures to be reached before the failure of the connections occurs (e.g., brittle failure), although in practical design this cannot be assumed but has to be proven.

This means that, in practice, and while the existing system-based direct design recommendations do not feature joint failure, it is necessary to separate the design of connections and to verify that they are sufficiently flexible to accommodate the induced rotations and capable of transferring the required internal forces (axial forces, shear forces and bending moments). Therefore, the ductility and resistance of connections needs to be checked according to current design specifications such as EN 1993-1-8 [46] after the members comprising the structure have been designed using system-based direct analysis. Designers should verify that the connections do not fail under the predicted frame capacities and demonstrate that they possess sufficient ductility for the frame ultimate limit states to be reached.

Research is currently underway to incorporate joint failure to system-based direct design approaches through a detailed modelling of the joint, from which it will be possible to check the resistance of connections directly from the advanced analysis without requiring further verifications using design specifications.

10. CHARACTERISTIC (NOMINAL) SYSTEM RESISTANCE

10.1. INTRODUCTION

The characteristic (nominal) system resistance R_k and deflections necessary to perform design checks when designing stainless steel structures using system-based direct design methods should be obtained from the nominal models built following the requirements prescribed in relevant standards such as prEN 1993-1-14 [4].

In addition to accurately modelling the material behaviour, initial geometric imperfections, residual stresses and connection behaviour, which have been extensively described in the previous Chapters, it is necessary to carry out an advanced analysis that accounts for all the relevant nonlinearities on the developed models to guarantee an accurate estimation of the resistance and stiffness of the system. This Chapter provides an overview of the different types of structural analysis available and establishes the analysis type that should be carried out when using the system-based direct design approach, in addition to some recommendations on how the characteristic (nominal) system resistance and deflections should be obtained from the load–displacement curves estimated numerically.

10.2. STRUCTURAL ANALYSIS TYPES

The most basic structural analysis type is the linear bifurcation analysis (LBA), in which the modes for which the structure buckles in different deformed shapes are determined in addition to the elastic critical bifurcation loads. This analysis assumes a linear elastic material model and no change of geometry before bifurcation. The remaining structural analysis types result from the consideration of the two typical nonlinearities present in the response of steel structures: geometric and material nonlinearities. Geometric nonlinearities arise from the appearance of moderate-to-large displacements and rotations in the structure, while material nonlinearities are a consequence of a nonlinear stress–strain relationship characterizing the material.

Depending on whether geometric nonlinearities are accounted for in the structural analysis, two types of analyses can be differentiated:

- First-order analysis: the analysis assumes that displacements and rotations are infinitesimal (i.e., establishes equilibrium in the undeformed configuration).

- Second-order analysis: the analysis establishes equilibrium in the deformed configuration of the structure and accounts for the effects of moderate-to-large displacements and rotations.

On the other hand, two additional analysis types are discerned depending on whether material nonlinearities are accounted for:

- Elastic analysis: the analysis assumes perfectly elastic material properties.
- Inelastic analysis: the analysis incorporates the effect of yielding or the nonlinear material behaviour.

The combination of the two classifications results in the following structural analysis types:

- First-order (linear) elastic analysis (LA): the analysis assumes perfectly elastic material properties and a first-order analysis, considering infinitesimal displacements and establishing equilibrium in the undeformed configuration of the structure.
- First-order inelastic analysis (MNA): the analysis assumes a first-order analysis (establishes equilibrium in the undeformed configuration of the structure) and an elastic-plastic material behaviour.
- Second-order elastic analysis (GNA): the analysis assumes a second-order analysis (establishes equilibrium in the deformed configuration of the structure) and perfectly elastic material properties.
- Second-order inelastic analysis (GMNA): the analysis assumes a second-order analysis (establishes equilibrium in the deformed configuration of the structure) and an elastic-plastic (or nonlinear) material behaviour.

When the consideration of the two types of nonlinearities is combined with the definition of initial imperfections (initial geometric imperfections and residual stresses), a fifth type of structural analysis can be defined, the second-order inelastic analysis with imperfections (GMNIA analysis), which is also known as advanced analysis.

Figure 14 illustrates the typical load–displacement curves corresponding to the different structural analysis types performed on the same structure.

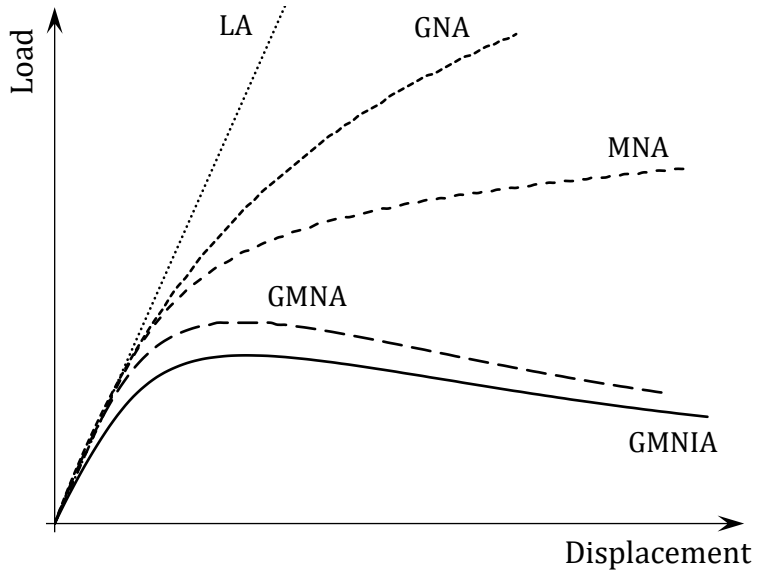

Figure 14. Graphical illustration of the structural responses arising from different structural analysis types.

While the structural analysis type typically adopted in the traditional *two-step* design approach is the second-order elastic analysis (GNA), first-order inelastic analysis (MNA) may also be carried out for the global plastic analysis of steel structures with compact cross-sections (i.e., definition of global plastic mechanisms). Conversely, the analysis type required when carrying out a system-based direct design of structures is the second-order inelastic analysis with imperfections (i.e., GMNIA analyses), or advanced analysis, in which the analysis incorporates all nonlinearities and the effects that may influence the response of the system (i.e., initial geometric imperfections, residual stresses, actual response of connections). Second-order inelastic analyses with imperfections (i.e., GMNIA analyses) are capable of accurately predicting the stiffness and resistance of stainless steel structures, in addition to displacements, internal forces and stresses, and can be used in system-based direct design approaches.

10.3. DETERMINATION OF THE CHARACTERISTIC (NOMINAL) SYSTEM RESISTANCE

The characteristic (nominal) resistance of the system R_k to be used in the Ultimate Limit State resistance checks when adopting system-based direct design approaches can be directly obtained from the load–displacement curve derived from an advanced analysis (i.e., second-order inelastic analysis with imperfections – GMNIA). If the load–displacement curve exhibits a clear peak load, typically for those cases in which the

failure of the system is governed by instability, this peak load is assumed as the nominal resistance of the system.

Nevertheless, when the failure of the frames is governed by yielding the load–displacement curve may not exhibit a clear peak load, especially when beam-type finite elements are adopted for the analysis. In such cases, the characteristic resistance R_{k} can be obtained as the load at which the stiffness of the curve falls below 5% of the initial stiffness or, alternatively, through the application of certain strain limits, following the approach prescribed in the Annex C of prEN 1993-1-14 [4]. Whereas the first procedure is very simple, the strain limit approach may provide a more accurate estimation of the characteristic resistance of the system but requires further calculations. Strain limits are also valid to simulate cross-section failure due to local buckling in beam-type finite element models, for example when systems comprised by slender cross-sections prone to local failure are designed.

Currently, the applicability of this strain limit approach is limited to doubly-symmetric I- and H-sections and square or rectangular hollow sections. The design value of the maximum longitudinal compressive strain $\varepsilon_{\mathrm{Ed}}$ at each cross-section shall satisfy

$$\varepsilon_{\mathrm{Ed}} \leq \varepsilon_{\mathrm{csm}} \qquad \text{Eq. 31}$$

where $\varepsilon_{\mathrm{Ed}}$ is the design value of the maximum longitudinal compressive strain and $\varepsilon_{\mathrm{csm}}$ is the limiting strain. It should be noted that the design value of $\varepsilon_{\mathrm{Ed}}$ may be taken as the maximum value averaged over a length of member equal to the elastic local buckling half-wavelength $L_{\mathrm{b,cs}}$, which can be determined numerically or using the expressions defined in [47], in order to account for the effect of local moment gradients. The limiting strain $\varepsilon_{\mathrm{csm}}$ is the Continuous Strength Method (CSM) strain limit, given by Eq. 32 and Eq. 33 for fully effective and slender cross-sections, respectively, when a rounded material model similar the two-stage Ramberg-Osgood model reported in Chapter 6 is adopted in the analysis.

$$\frac{\varepsilon_{\mathrm{csm}}}{\varepsilon_{\mathrm{y}}} = \frac{0.25}{\bar{\lambda}_{\mathrm{p,cs}}^{\,3.6}} + \frac{0.002}{\varepsilon_{\mathrm{y}}} \leq \Omega \qquad \text{for} \qquad \bar{\lambda}_{\mathrm{p,cs}} \leq 0.68 \qquad \text{Eq. 32}$$

$$\frac{\varepsilon_{csm}}{\varepsilon_y} = \left(1 - \frac{0.222}{\bar{\lambda}_{p,cs}^{1.05}}\right)\frac{1}{\bar{\lambda}_{p,cs}^{1.05}} + \frac{0.002(\sigma/f_y)^n}{\varepsilon_y} \quad \text{for } 0.68 < \bar{\lambda}_{p,cs} < 1.00 \qquad \text{Eq. 33}$$

In Eq. 32 Ω is a project specific parameter that defines the maximum permissible level of plastic strain in the structure, which adopts the recommended value of 15 unless the National Annex gives a different value, and $\bar{\lambda}_{p,cs}$ is the local slenderness of the full cross-section, determined from Eq. 34, in which $\sigma_{cr,cs}$ is the elastic local buckling stress of the full cross-section.

$$\bar{\lambda}_{p,cs} = \sqrt{f_y/\sigma_{cr,cs}} \qquad \text{Eq. 34}$$

Different alternatives exist to estimate the elastic local buckling stress of the full cross-section $\sigma_{cr,cs}$:

- conservatively adopt $\bar{\lambda}_{p,cs}$ as the plate slenderness $\bar{\lambda}_p$ of the most slender element comprising the cross-section, according to EN 1993-1-5 [48],
- use the simple analytical expressions for determining $\sigma_{cr,cs}$ for full cross-sections proposed in [49],
- use finite strip software such as CUFSM [50], or
- use advanced finite element software.

Figure 15 illustrates the definition of the characteristic (nominal) resistance of the system R_k from the load–displacement curve for different scenarios, including response curves in which the peak load is not discernible (Frame A) and curves with a clear peak load (Frame B). For Frame A the load factors corresponding to the 5% initial stiffness reduction and the CSM strain limit approaches are shown, which result in slightly different load factors for the analysed case. While the load factor resulting from the application of the CSM strain limits is 6% higher, the 5% initial stiffness reduction approach is much simpler to adopt as it does not require performing the calculations detailed above in this Section.

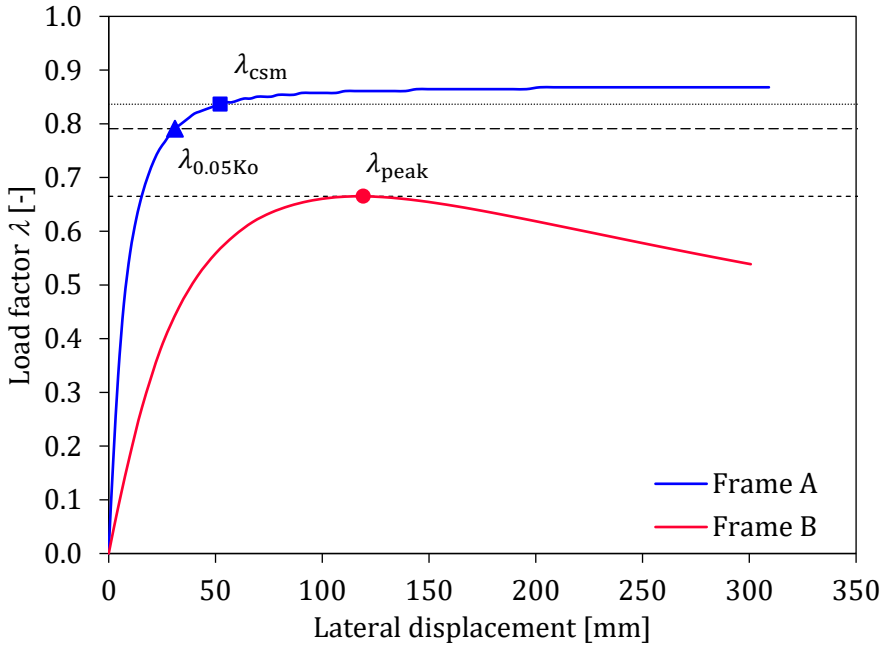

Figure 15. Graphic definition of the different approaches to determine R_k with (or in the absence of) a peak load in the load–displacement curve.

10.4. DETERMINATION OF DEFLECTIONS

Deflections and lateral displacements for the Serviceability Limit State checks should be also determined from a second-order inelastic analysis with imperfections (i.e., GMNIA analysis) similar to that adopted in the estimation of the characteristic (or nominal) system resistance. Deflections should be estimated using the same advanced finite element model that includes initial geometric imperfections, residual stresses and the actual response of connections, considering both geometric and material nonlinearities in the analysis, since all these features may affect the stiffness of structural systems. Deflections and lateral displacements should be, however, determined considering the load combinations relevant to the Serviceability Limit State under consideration, as specified in prEN 1990 [23] and discussed in Chapter 2.

11. CASE STUDIES

11.1. INTRODUCTION

This Section presents two case studies on cold-formed stainless steel portal frames through which the application of the system-based direct design (and verification) procedure is illustrated. Frame 1 features cold-formed rectangular hollow sections made from austenitic stainless steel material, and subjected to gravity loads only. The frame geometry is defined so that its design is determined from strength requirements (i.e., Ultimate Limit State (ULS) governing criteria). Alternatively, Frame 2 is made from a basic duplex stainless steel alloy and loaded with a combination of permanent gravity and wind loads. Also comprised by cold-formed rectangular hollow sections, Frame 2 is defined so that its design is governed by serviceability requirements (i.e., Serviceability Limit State (SLS) criteria).

For each case study, the frame geometry, material properties and loads are presented first, followed by a detailed description of the advanced finite element model built using the general purpose software ABAQUS [41]. The two frames are then designed attending to resistance and serviceability criteria using the system-based direct design approach featured in this recommendation document and the final cross-sections are presented. Finally, the resulting cross-sections are compared with those derived using the traditional *two-step* design approach prescribed in the Eurocode prEN 1993-1-4 [21] and some concluding remarks are presented.

11.2. BRIEF OVERVIEW OF EUROCODE PROVISIONS

This Section presents a brief overview of the provisions prescribed in prEN 1993-1-4 [21] for the design of stainless steel structures, which includes the supplementary provisions necessary to account for the different behaviour exhibited by stainless steel alloys for strength and serviceability considerations.

11.2.1. Design for Strength

Since the response and strength of stainless steel structures can be significantly affected by second-order effects and material nonlinearities, it is important to evaluate whether these will be relevant in the performance of the structure under consideration to guarantee that the appropriate analysis type is carried out when determining internal forces.

The susceptibility of stainless steel structures to second-order effects is evaluated through the consideration of the modified critical load factor $\alpha_{\mathrm{cr,mod}}$, similar to what is prescribed in EN 1993-1-1 [24] for steel structures, but which also allows accounting for the loss of stiffness due to material nonlinearities in the global stability of frames. According to §7.4.3.1(2) of prEN 1993-1-4 [21], first-order theory may be used when determining the internal forces when $\alpha_{\mathrm{cr,mod}} \geq 10$, which can be determined from Eq. 35,

$$\alpha_{\mathrm{cr,mod}} = \alpha_{\mathrm{cr}} Y \, K_{\mathrm{s}}/K \qquad \text{Eq. 35}$$

where α_{cr} is the factor by which the design load should be increased to cause a sway elastic instability, Y is a factor that considers the further loss of stiffness due to second-order effects and K_{s}/K is the ratio of the secant lateral stiffness to the initial lateral stiffness of the structure at the design load. The α_{cr}-factor can be determined from an elastic buckling analysis, the values of the Y-factor (calibrated in [51] and adopted in prEN 1993-1-4 [21]) are reported in Table 10, and the K_{s}/K ratio can be expressed in terms of displacements as $\Delta_{\mathrm{el}}/\Delta_{\mathrm{pl}}$, in which Δ_{el} is the displacement at the design load considering a linear elastic analysis (LA) and Δ_{pl} is the displacement corresponding to a first-order inelastic analysis (MNA).

Table 10. Values of the Y-parameter prescribed in prEN 1993-1-4 [21].

Stainless steel family	Single storey portal frames	All other frames
Austenitic	0.80	0.55
Duplex	0.85	0.60
Ferritic	0.90	0.65

The relevance of the material nonlinearity in the design of stainless steel structures is evaluated through the $E_{\mathrm{s}}/E \geq 0.2$ relationship provided in §7.4.2 of prEN 1993-1-4 [21], which defines the limit below which the response of all members contributing to the global stability can be considered as predominantly elastic, and an elastic global analysis can be carried out. E_{s} is the secant modulus corresponding to the maximum stress σ_{Ed} obtained from a first-order elastic analysis under the design loads, given by Eq. 36, and the basic material parameters E, f_{y} and n are as defined in Chapter 6.

$$E_s = \frac{E}{1 + 0.002 \frac{E}{\sigma_{Ed}} \left(\frac{\sigma_{Ed}}{f_y}\right)^n} \quad \text{Eq. 36}$$

Once the analysis type necessary for the estimation of internal design forces is determined and performed considering all the relevant initial imperfections, the resistance of cross-sections and members needs to be checked as per in the *two-step* design approach using the partial safety factors for cross-section and member resistance equal to $\gamma_{M0} = 1.10$ and $\gamma_{M1} = 1.10$, respectively, and the resistance equations prescribed in prEN 1993-1-4 [21].

Cross-section and member resistances can be calculated from the traditional equations given in §8 of prEN 1993-1-4 [21], which are based on the yield stress of the material, or using the Continuous Strength Method (CSM) design expressions included in the Annex B of prEN 1993-1-4 [21], with which is possible to account for the effect of strain hardening in cross-sectional resistance verifications.

11.2.2. Design for Serviceability

The effects of the nonlinear stress–strain response of stainless steel alloys should be taken into account when estimating deflections. According to §9.2 of prEN 1993-1-4 [21], deflections should be determined from a linear elastic analysis but using the secant modulus of elasticity $E_{s,ser}$ instead of the Young's modulus E, which can be estimated from Eq. 37,

$$E_{s,ser} = \left(E_{s,1} + E_{s,2}\right)/2 \quad \text{Eq. 37}$$

where $E_{s,1}$ and $E_{s,2}$ are the secant moduli corresponding to the stress in the tension flange $\sigma_{Ed,1}$ and the stress in the compression flange $\sigma_{Ed,2}$, respectively, under the service design loads, determined from Eq. 36. Since the value of the secant modulus $E_{s,ser}$ will typically vary along the length of the member, as the stress distribution will not be uniform, it is possible to adopt a conservative approach in which the minimum value of $E_{s,ser}$ corresponding to the maximum values of the $\sigma_{Ed,1}$ and $\sigma_{Ed,2}$ stresses are adopted throughout the members.

11.3. CASE STUDY 1: STAINLESS STEEL PORTAL FRAME UNDER GRAVITY LOADS

11.3.1. General

The stainless steel portal frame analysed in this example (Frame 1) is a single bay and single storey pitched frame comprising cold-formed Rectangular Hollow Sections (RHS) with a span length of 6 m, a column height of 3.5 m and a total height of 4 m, as shown in Figure 16, with fixed-ended column bases and rigid connections at the eaves and apex joints.

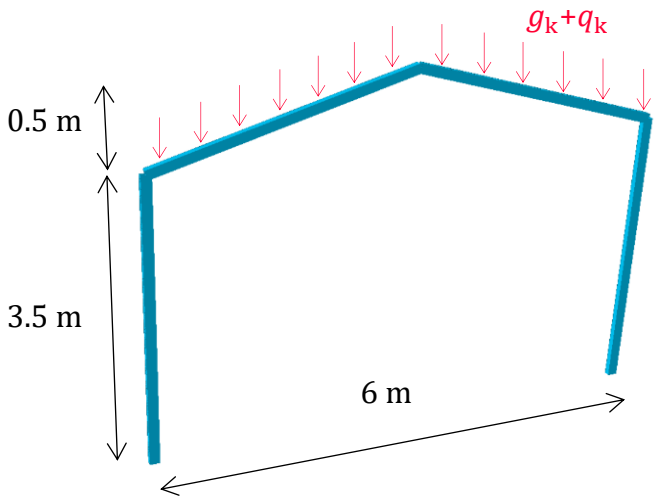

Figure 16. Layout and load definition for Frame 1.

Frame 1 is made from the austenitic stainless steel grade 1.4301, whose basic nominal properties of the unformed material (E, f_y, f_u and n) according to prEN 1993-1-4 [21] are reported in Table 11. The remaining parameters (i.e., m and ε_u) are estimated using the predictive equations prescribed in [34] and summarized in Chapter 6. It should be noted that in this example the strength enhancement due to the cold forming of the cross-sections has been accounted for through the models prescribed in prEN 1993-1-4 [21] and reported in Section 6.2. This means that, since the enhancement models depend on the areas of the corner-to-flat regions (see Section 6.2), different enhanced material properties are adopted for each cross-section considered in the analysis for each iteration.

Table 11. Nominal material properties for stainless steel grade 1.4301 (Frame 1).

Material parameter	E	f_y	f_u	n	m	ε_u
Value	200,000 MPa	230 MPa	550 MPa	7	2.2	58%

The frame is subjected to gravity loads only: a characteristic permanent load of g_k=2.0 kN/m that includes the self-weight, roof cladding and secondary steelwork, and an imposed (live) load of q_k=6.0 kN/m according to EN 1991-1-1 [52] applied at the rafters, as shown in Figure 16.

11.3.2. Development of the nominal advanced model

The advanced finite element model is built using the general purpose software ABAQUS [41] following the requirements discussed in Chapters 5 to 9 and the geometric and material properties defined in Section 11.3.1. Initial geometric imperfections are introduced as a linear combination of six buckling modes, which have been obtained from a prior linear bifurcation analysis (LBA), and the corresponding imperfection amplitudes determined from Eq. 30: A_1=4.8 mm, A_2=1.1 mm, A_3=1.6 mm, A_4=1.6 mm, A_5=1.1 mm and A_6=1.1 mm. Residual stresses are introduced using the SIGINI subroutine [41].

Material properties are input through user-defined nonlinear true stress *vs* true plastic strain relationships using the engineering enhanced material properties based on the values reported in Table 11 and Eq. 24-Eq. 25. Rigid joints are considered for the apex and eaves connections, fixed-ended conditions are imposed at the column bases and the design loads are introduced at the rafters as line loads. The frame is discretised using the linear beam-type finite element B21 available in the ABAQUS library [41], since the behaviour of the frame is limited to the in-plane response, and the selected mesh corresponded to a typical element size of 100 mm. Figure 17 shows the advanced finite element model built for Frame 1, in which the boundary conditions and the applied gravity loads are illustrated.

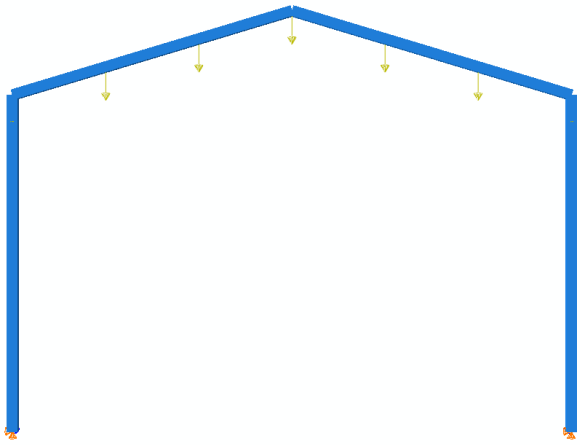

Figure 17. General layout of the advanced finite element model for Frame 1.

11.3.3. Ultimate Limit State checks

Assuming the load factors prescribed in prEN 1990 [23] for ULS, γ_G=1.35 for permanent loads and γ_Q=1.50 for imposed live loads, the resulting design load is p_{Ed}=11.7 kN/m. Once the advanced finite element is built and the design loads are applied, fully nonlinear analyses (i.e., GMNIA analyses) are run, from which the corresponding load factor–vertical deflection curve is obtained. The final solution for the frame design is obtained by iterating on the cross-section dimensions until the design check given in Eq. 5 is satisfied.

For the first iteration the 130×80×4 cross-section is selected, in which the H×B×t notation refers to the height H, width B and thickness t of the RHS cross-section. The load factor–vertical apex deflection curve for the 130×80×4 cross-section is shown in Figure 18, together with the suitable system partial safety factor $\gamma_{M,s}$ for the ULS design check given in Table 3.

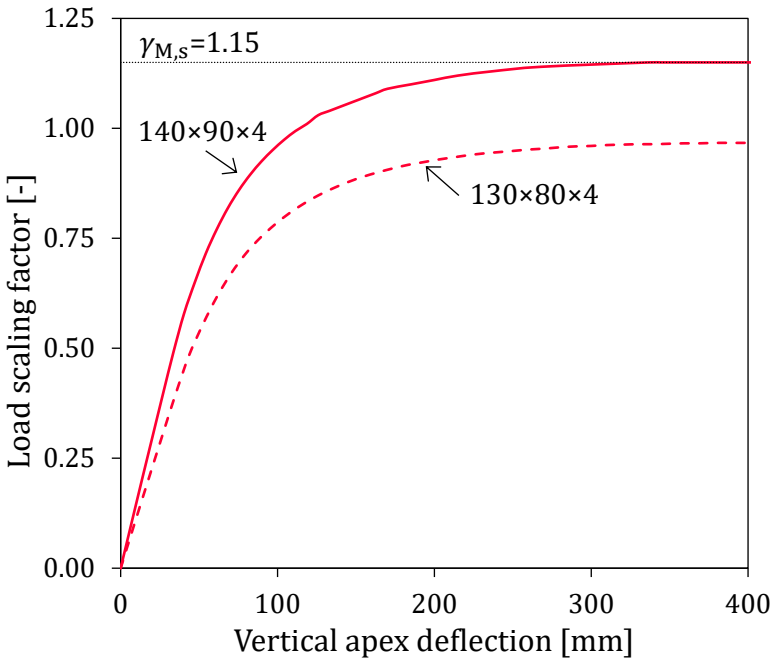

Figure 18. Load scaling factor–vertical apex deflection curves for different cross-sections and ULS design check for Frame 1.

From the results shown in Figure 18, the ultimate load factor is determined as the maximum load scaling factor (i.e., the peak load of the load factor–deflection curve), which for the 130×80×4 cross-section is λ_u=0.97. In this case the ultimate load factor is lower than the corresponding system partial safety factor, indicating that the selected cross-section is not suitable for the design loads and frame geometry adopted.

$$\lambda_u = 0.97 < \gamma_{M,s} = 1.15$$

Thus, additional iterations are required until a cross-section for which the $\lambda_u \geq \gamma_{M,s}$ condition is fulfilled is found, for example the cross-section 140×90×4. The load factor–vertical apex deflection curve for this cross-section is also shown in Figure 18, which presents an ultimate load factor of λ_u=1.15, satisfying the ULS design check.

$$\lambda_u = 1.15 = \gamma_{M,s} = 1.15 \checkmark$$

11.3.4. Serviceability Limit State checks

The Serviceability Limit State (SLS) check of the portal frame should be performed using the advanced model described in Section 11.3.2 but assuming the serviceability design loads. The SLS check for steel frames subjected to gravity loads refers to the vertical deflection of the apex section considering an allowable deflection limit of $\delta_a = s/125$ under imposed loads only [23], with s being the span of the frame. Adopting a load factor γ_Q=1.0, according to prEN 1990 [23], the serviceability design load is p_{Ed}=6.0 kN/m and the corresponding load factor–vertical deflection curve for the cross-section 140×90×4 resulting from Ultimate Limit State design is presented in Figure 19.

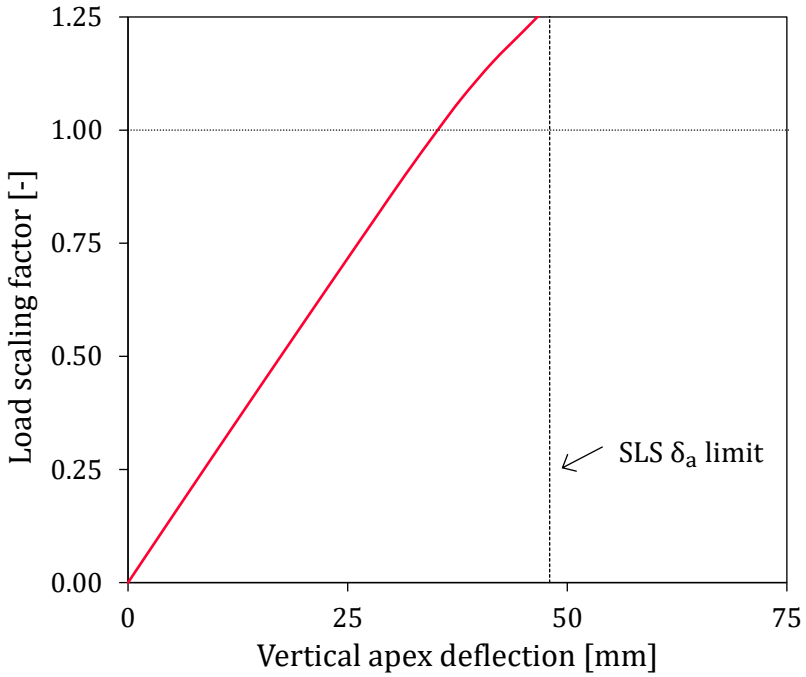

Figure 19. Load scaling factor–vertical apex deflection curve under the SLS design load for the cross-section resulting from ULS design for Frame 1.

For a load factor equal to unity (i.e., serviceability design load p_{Ed}), the vertical deflection predicted by the advanced FE model at the apex section is Δ_{v}=35.3 mm, with is lower than the allowable deflection limit ($\delta_{\mathrm{a}} = 48\ mm$), and thus it can be concluded that strength is the governing criteria for Frame 1 and that serviceability requirements are satisfied without requiring a re-design of the frame.

$$\Delta = 35.3\ mm < \delta_{\mathrm{a}} = 48\ mm \ \checkmark$$

11.3.5. Comparison with the traditional two-step design approach

This Section presents the comparison of the frame designed using a system-based direct design approach with the cross-section resulting from the adoption of the *two-step* provisions codified in prEN 1993-1-4 [21] and summarized in Section 11.2. Both resistance and serviceability considerations are taken into account, and the final solutions are compared in terms of required material consumption.

According to §7.4.3.1 and §7.4.2 of prEN 1993-1-4 [21], and considering the design loads, geometric properties and material characteristics of Frame 1, it is necessary to account for material and geometric nonlinearities in the estimation of the internal design forces. Since the columns in Frame 1 are subjected to significantly low compressive forces, the required cross-section dimension is determined by the flexural capacity of the section. Considering that the limiting check for the member-based *two-step* design approach is the bending capacity of the cross-section, two different alternatives are analysed: the adoption of a flexural capacity based on the yield stress of the material and a flexural resistance that accounts for strain hardening effects, adopting the Continuous Strength Method (CSM) bending moment capacity prescribed in the Annex B of prEN 1993-1-4 [21].

The cross-sections resulting from the member-based *two-step* prEN 1993-1-4 [21] design of Frame 1 for Ultimate Limit State considerations are 155×95×4 and 140×90×4 when the bending moment capacity is limited to the yield stress f_{y} and when strain hardening is considered, respectively. The different optimized cross-sections are summarized in Table 12, where the differences in material consumption, relative to the area of the cross-section corresponding to the system-based direct design approach, are also reported.

Table 12. Comparison of minimum cross-section requirements for different design approaches for Frame 1.

Design approach	Ultimate Limit State (ULS)		Serviceability Limit State (SLS)	
	Required cross-section	Difference in material	Required cross-section	Difference in material
System-based direct design	140×90×4	–	140×90×4	–
Two-step approach (limited to f_y)	155×95×4	+9.2%	150×90×4	+4.6%
Two-step approach (considering strain hardening)	140×90×4	0.0%	150×90×4	+4.6%

From these results it is evident that considering strain hardening effects in the prediction of the cross-sectional resistance results in a more efficient design for Frame 1. For this particular frame the required cross-section using the system-based direct approach and that resulting from the traditional *two-step* approach (considering strain hardening) are the same due to the fact that in the two cases equivalent fully nonlinear structural analyses are carried out and that even if the CSM expression for the flexural capacity inevitably presents some conservatism, the partial safety factor assumed in the cross-section check (i.e., $\gamma_{M0} = 1.10$) is less conservative than that used in the system-based direct approach (i.e., $\gamma_{M,s} = 1.15$). These two effects effectively compensate each other, and the resulting cross-sections are the same.

Regarding the Serviceability Limit State, the vertical deflections at the apex section are estimated using the secant modulus of elasticity $E_{s,ser}$ approach for the *two-step* prEN 1993-1-4 [21] design approach. The resulting secant modulus for Frame 1 is around $E_{s,ser}$=160,000 MPa, which corresponds to a $E_{s,ser}/E$ ratio of 0.80, indicating that the frame is significantly affected by material nonlinearities even for service design loads. The required cross-sections for the different design approaches for SLS are also summarized in Table 12, which shows that larger cross-sections are necessary for the *two-step* approach than for the system-based direct design approach. These results suggest that the secant modulus approach is slightly more conservative than the adoption of the actual stress-strain behaviour of the material for a system-based direct design.

11.4. CASE STUDY 2: STAINLESS STEEL PORTAL FRAME UNDER GRAVITY PLUS WIND LOADS

11.4.1. General

The portal frame analysed in this second example (Frame 2) is also a single bay single storey pitched frame comprising stainless steel cold-formed Rectangular Hollow Sections (RHS). The total height of the frame is 6 m, while the height of the columns is equal 4.8 m and the span length is 8 m, as shown in Figure 20. The frame bases are also fixed-ended and rigid connections are assumed at the eaves and apex joints.

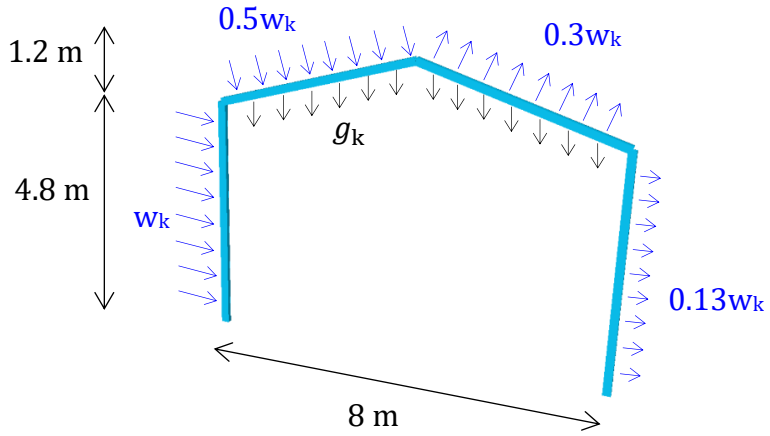

Figure 20. Layout and load definition for Frame 2.

Frame 2 is made from the common duplex grade 1.4462, the basic nominal properties of which (E, f_y, f_u and n), according to prEN 1993-1-4 [21], are reported in Table 13 for the unformed material. The remaining parameters (i.e., m and ε_u) are estimated using the predictive equations prescribed in [34] and summarized in Chapter 6. As for Frame 1, the strength enhancements due to the cold forming of the cross-sections according to the model prescribed in prEN 1993-1-4 [21] has been considered in the material properties introduced in the advanced finite element models and updated on each iteration.

Table 13. Nominal material properties for stainless steel grade 1.4462 (Frame 2).

Material parameter	E	f_y	f_u	n	m	ε_u
Value	200,000 MPa	500 MPa	700 MPa	8	3	28.6%

Frame 2 is subjected to a combination of a permanent gravity load of g_k=2.0 kN/m at the rafters and to the wind load pattern shown in Figure 20. The wind load has been

determined from prEN 1991-1-4 [53] for a basic wind speed of v_0=29 m/s and a Terrain Category II, which results in a characteristic wind load of w_k=5.85 kN/m.

11.4.2. Development of the nominal advanced model

The general purpose software ABAQUS [41] is also used to build the advanced finite element model for Frame 2, adopting the same features described in Section 11.3.2 but adapted to the geometry and material properties of the new frame. Material properties are defined through user-defined nonlinear true stress *vs* true plastic strain relationships using the enhanced material properties based on the basic values reported in Table 13, and residual stresses are introduced using the SIGINI subroutine following the model reported in Section 8.1 for cold-formed stainless steel rectangular hollow sections.

The connections at the apex and eaves joints are considered rigid, while fixed-ended conditions are imposed at the column bases. Permanent loads are input as a line load in the rafters and the wind load is introduced as a set of pressure loads at the columns and rafters. Gravity loads are introduced first and a fully nonlinear analysis is carried out. On a second step, the wind loads are applied incrementally until the collapse of the frame is reached, also using a fully nonlinear analysis. Regarding initial geometric imperfections, these are based on the linear superposition of six buckling modes amplified using the amplitudes determined from Eq. 30, which for Frame 2 are A_1=7.2 mm, A_2=1.8 mm, A_3=2.7 mm, A_4=2.7 mm, A_5=1.8 mm and A_6=1.8 mm. The shape of the buckling modes is determined from a prior linear bifurcation analysis (LBA).

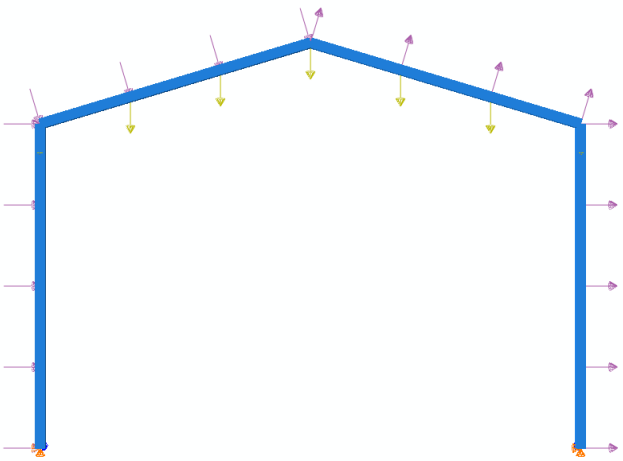

Figure 21. General layout of the advanced finite element model for Frame 2.

The advanced finite element model built for Frame 2 is shown in Figure 21, in which the applied loads and the boundary conditions are illustrated. The linear beam-type B21

finite elements available at the ABAQUS library [41] are adopted to discretise the portal frame, with a typical element size of 100 mm. Only the in-plane response of the frame is considered for Frame 2.

11.4.3. Ultimate Limit State checks

Adopting the load factors prescribed in prEN 1990 [23] for ULS (i.e., γ_G=1.35 and γ_w=1.50), the resulting design permanent and wind loads are g_{Ed}=2.7 kN/m and w_{Ed}=8.78 kN/m. Considering this design loads, a fully nonlinear analysis (i.e., GMNIA analysis) is run until a suitable cross-section satisfying the ULS design check given in Eq. 5 is found iteratively. The resulting RHS cross-section is 150×90×4.

Figure 22 presents the wind load factor–lateral apex displacement curve, also showing the corresponding system partial safety factor $\gamma_{M,s}$ calibrated for stainless steel frames for the ULS design check under gravity plus wind load conditions, as reported in Table 3.

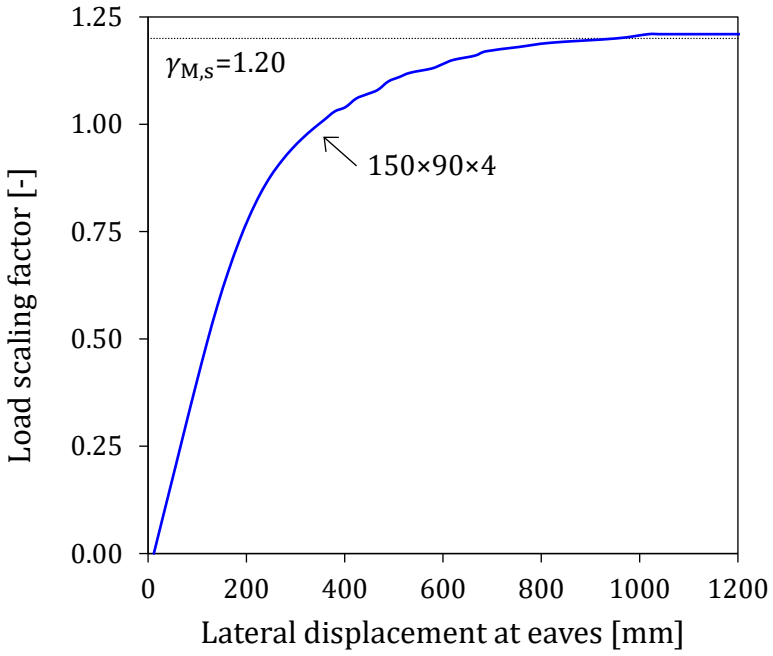

Figure 22. Load scaling factor–lateral displacement curve and ULS design check for Frame 2.

From the results shown in Figure 22, the ultimate wind load factor for the 150×90×4 cross-section is λ_u=1.21, obtained as the maximum (i.e., peak load), and which is higher than the corresponding system partial safety factor $\gamma_{M,s}$, indicating that the selected cross-section is suitable for the design loads and frame geometry considered.

$$\lambda_u = 1.21 > \gamma_{M,s} = 1.20 \quad \checkmark$$

11.4.4. Serviceability Limit State checks

In the case of systems subjected to lateral loads such as wind loading, the serviceability check usually refers to the lateral displacement or drift of the frame under the lateral loads. The allowable lateral displacement limit assumed for this example is $\delta_a = H/300$, where H is the height of the frame at the apex section, according to the limit adopted in [6,9]. Different allowable deflection limits can be found, nevertheless, in other codes and design manuals.

The serviceability check of the portal frame is carried out using the advanced FE model considered for ULS design, but adopting a design load corresponding to the serviceability load combination. Assuming load factors of γ_G=1.0 and γ_w=1.0, according to prEN 1990 [23], the serviceability design loads are p_{Ed}=2.0 kN/m and w_{Ed}=5.85 kN/m. The loads are also introduced in two steps: the gravity load p_{Ed} is introduced first carrying a GMNIA analysis, and the serviceability wind loads are then introduced incrementally through a fully nonlinear analysis. The wind load factor–lateral displacement curve for the cross-section resulting from ULS design (i.e., 150×90×4) is shown in Figure 23, where the allowable deflection limit δ_a is also indicated.

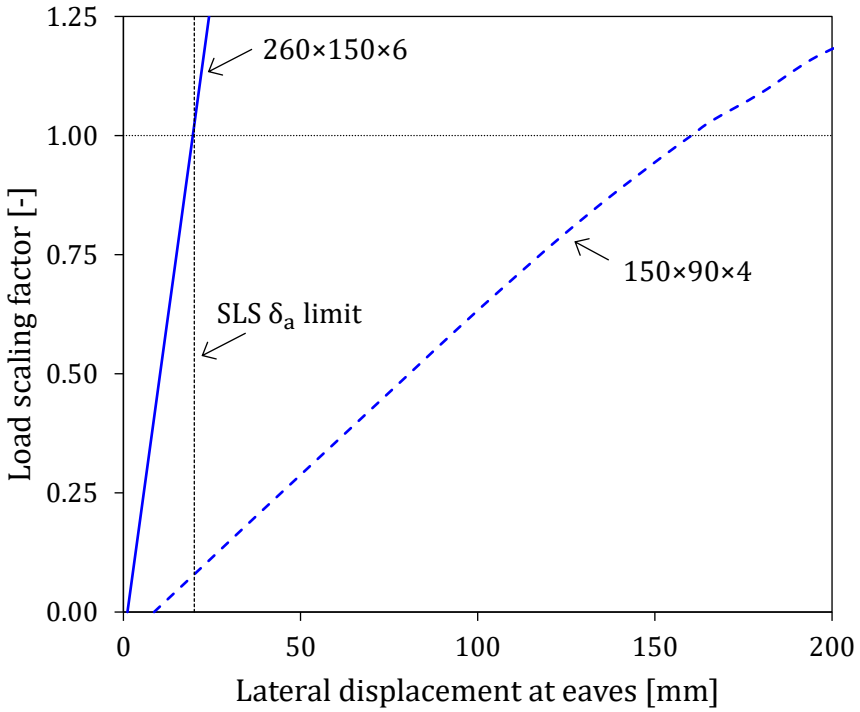

Figure 23. Load scaling factor–lateral displacement curves under the SLS design load for the cross-sections resulting from ULS and SLS designs for Frame 2.

It is evident from Figure 23 that the cross-section 150×90×4 is insufficient to meet the serviceability check under lateral wind loads because the lateral displacement at the service loads is remarkably larger than the allowable limit (δ_a=20 mm), so a re-design of the frame is necessary.

$$\Delta = 160\ mm > \delta_a = 20\ mm$$

Testing larger cross-sections iteratively until the serviceability check given in in Eq. 6 is fulfilled, the 260×150×6 cross-section can be selected for the serviceability design of Frame 2, which according to the wind load scaling factor–lateral displacement curve shown in Figure 23 meets the serviceability criteria.

$$\Delta = 19.6\ mm < \delta_a = 20\ mm \ \checkmark$$

11.4.5. Comparison with the traditional two-step design approach

As for Frame 1, this Section summarizes the solutions resulting from the adoption of the member-based *two-step* provisions codified in prEN 1993-1-4 [21] for strength and serviceability considerations, and compares the resulting cross-section with that obtained when the frame is designed using the system-based direct design approach.

In the case of Frame 2, and according to §7.4.3.1 and §7.4.2 of prEN 1993-1-4 [21], the design loads, geometric properties and material characteristics result in a non-sway elastic structure, and the internal design forces can be determined carrying out a linear elastic analysis of the structure. The design of Frame 2 is also governed by the flexural capacity of the critical cross-section, as the compressive forces at the columns are low. Hence, the two alternatives for determining the flexural capacity of the cross-sections considered for Frame 1 are also analysed herein for the member-based *two-step* design approach: the flexural capacity limited by the yield stress and the Continuous Strength Method (CSM) bending moment capacity accounting for strain hardening effects, as defined in the Annex B of prEN 1993-1-4 [21].

The cross-section required to withstand the design gravity plus wind load combination under the Ultimate Limit State considerations according to the *two-step* prEN 1993-1-4 [21] design approach is 150×100×5 when the bending moment capacity is limited to the yield stress f_y, and also when strain hardening is considered, since the cross-section has

a slenderness that is on the limit between Class 3 and Class 4 cross-sections, and thus cannot benefit from strain hardening when the CSM approach is adopted.

The sections corresponding to the different design approaches are reported in Table 14, which also indicates the differences in material consumption relative to the area of the cross-section resulting from the system-based direct design approach. In this case, the cross-sections required for the member-based *two-step* design approach are significantly larger than that obtained for the system-based direct design for Ultimate Limit State considerations (material reductions of nearly 30% are observed).

Table 14. Comparison of minimum cross-section requirements for different design approaches for Frame 2.

Design approach	Ultimate Limit State (ULS)		Serviceability Limit State (SLS)	
	Required cross-section	Difference in material	Required cross-section	Difference in material
System-based direct design	150×90×4	–	260×150×6	–
Two-step approach (limited to f_y)	150×100×5	+28.7%	260×150×6	+0.0%
Two-step approach (considering strain hardening)	150×100×5	+28.7%	260×150×6	+0.0%

To consider the Serviceability Limit State check for the *two-step* prEN 1993-1-4 [21] approach, the secant modulus of elasticity $E_{s,ser}$ approach is adopted. In this particular case the frame remains in the elastic range for the service design loads and a $E_{s,ser}/E$ ratio of 1.0 is obtained. Hence, there is no difference in using the actual stress–strain curve or the secant modulus approach, and the solutions for the system-based direct design approach and the *two-step* approach for serviceability are the same, the 260×150×6 cross-section reported in Table 14.

11.5. CONCLUDING REMARKS

The comparison of the cross-sections optimized for Frame 1 and Frame 2 following the member-based *two-step* design approach and the system-based direct design method demonstrates that the system-based direct approach results in a much simpler and faster verification process than the one adopted in prEN 1993-1-4 [21], and that significant reductions in material consumption can be achieved, leading to lighter and more

economical structural configurations. In system-based direct design methods it is not necessary to check whether geometrical and material nonlinearities are relevant to the structure under consideration and, since the verification procedure does not require checking the resistance of individual cross-sections and members, it is significantly simpler and faster.

Regarding serviceability considerations, the results presented in these two case studies indicate that the cross-sections required to meet the deflection criteria may be larger than those required for resistance considerations for the two design approaches. Hence, permitting larger deformations in Ultimate Limit State design through the adoption of system-based direct design approaches does not result in an additional negative effect on the final selected cross-section. This fact does, however, represent a limitation to the advantages presented by system-based direct design methods in terms of resistance prediction due to serviceability requirements.

Note that for the comparison of the member-based *two-step* and system-based direct design approaches presented in this Chapter only the strictly minimum cross-section differences have been determined, resulting in non-commercial height and width values. Therefore, the differences obtained between the two approaches would be larger in practice. It is also worth mentioning that the design of Frame 1 and Frame 2 is, according to the member-based *two-step* prEN 1993-1-4 [21] design approach, limited by the flexural capacity of the critical cross-sections. Hence, for those systems in which member failure modes are to be expected, the differences between the two design approaches are expected to be larger than those presented in this study because design equations for members tend to be more conservative than those prescribed for cross-sectional capacities in prEN 1993-1-4 [21].

REFERENCES

[1] Standards Australia (AS/NZS) (2020) AS/NZS 4100 *Steel Structures*. Sydney, Australia, 2020.

[2] Standards Australia (AS/NZS) (2018). AS/NZS 4600. *Cold-formed steel structures*. Sydney, Australia.

[3] American Institute of Steel Construction (ANSI/AISC) (2016) AISC 360. *Specification for Structural Steel Buildings*. Illinois, USA, 2016.

[4] Working Group 22 for Eurocode 3, CEN/TC 250/SC3/WG22 (2022) *prEN 1993-1-14. Eurocode 3: Design of steel structures – Part 1-14: Design assisted by finite element analysis*. Final Document. Brussels, Belgium.

[5] Zhang, H.; Liu, H.; Ellingwood, B.R.; Rasmussen, K.J.R. (2018) *System reliabilities of planar gravity steel frames designed by the inelastic method in AISC 360-10*. Journal of Structural Engineering (ASCE) 144(3), 04018011.

[6] Zhang, H.; Ellingwood, B.R.; Rasmussen, K.J.R. (2014) *System reliabilities in steel structural frame design by inelastic analysis*. Engineering Structures 81, 341–348.

[7] Zhang, H.; Shayan, S.; Rasmussen, K.J.R.; Ellingwood, B.R. (2016) *System-based design of planar steel frames, I: Reliability framework*. Journal of Constructional Steel Research 123, 135–143.

[8] Zhang, H.; Shayan, S.; Rasmussen, K.J.R.; Ellingwood, B.R. (2016) *System-based design of planar steel frames, II: Reliability results and design recommendations*. Journal of Constructional Steel Research 123, 154–161.

[9] Liu, W.; Zhang, H.; Rasmussen, K.J.R. (2018) *System reliability-based Direct Design Method for space frames with cold-formed steel hollow sections*. Engineering Structures 166, 79–92.

[10] Sena Cardoso, F.; Zhang, H.; Rasmussen, K.J.R.; Yan, S. (2019) *Reliability calibrations for the design of cold-formed steel portal frames by advanced analysis*. Engineering Structures 182, 164–171.

[11] Sena Cardoso, F.; Zhang, H.; Rasmussen, K.J.R. (2019) *System reliability-based criteria for the design of steel storage rack frames by advanced analysis: Part II – Reliability analysis and design applications*. Thin-Walled Structures 141, 725–739.

[12] Wang, C.; Zhang, H.; Rasmussen, K.J.R.; Reynolds, J.; Yan, S. (2020) *Reliability-based limit state design of support scaffolding systems*. Engineering Structures 216, 110677.

[13] New Generation Design Methods for Stainless Steel Structures (NewGeneSS). Marie Sklodowska-Curie Fellowship 2018, funded by the European Union's Horizon 2020 Research and Innovation Programme under Grant Agreement No. 842395.

[14] Arrayago, I.; Rasmussen, K.J.R.; Real, E. (2020) *Statistical analysis of the material, geometrical and imperfection characteristics of structural stainless steels and members*. Journal of Constructional Steel Research 175, 106378.

[15] Arrayago, I.; Rasmussen, K.J.R. (2021) *System-based reliability analysis of stainless steel frames under gravity loads*. Engineering Structures 231, 111775.

[16] Arrayago, I.; Rasmussen, K.J.R.; Zhang, H. (2022) *System-based reliability analysis of stainless steel frames subjected to gravity and wind loads*. Structural Safety 97, 102211.

[17] Arrayago, I.; Rasmussen, K.J.R. (2022) *Reliability of stainless steel frames designed using the Direct Design Method in serviceability limit states*. Journal of Constructional Steel Research 196, 107425.

[18] American Institute of Steel Construction (ANSI/AISC) (2021) AISC 370. *Specification for Structural Stainless Steel Buildings*. Illinois, USA, 2021.

[19] American Society of Civil Engineers (ASCE). SEI/ASCE 8. *Specification for the Design of Cold-Formed Stainless Steel Structural Members*. Virginia, USA, 2022.

[20] Standards Australia (AS/NZS). AS/NZS 4673. *Cold-formed stainless steel structures*. Sydney, Australia, 2001.

[21] European Committee for Standardization (CEN) (2020) prEN 1993-1-4. *Eurocode 3: Design of Steel Structures – Part 1-4: General Rules. Supplementary Rules for Stainless Steels*. Final Document. Brussels, Belgium.

[22] Arrayago, I.; Rasmussen, K.J.R.; Zhang, H.; Real, E. (2022) *On the development of the system-based direct design approach for stainless steel frames using advanced analysis*.

Proceedings of the Sixth International Experts Seminar on Stainless Steel in Structures. London, United Kingdom.

[23] European Committee for Standardization (CEN) (2020) prEN 1990. *Eurocode: Basis of Structural Design*. Draft Document. Brussels, Belgium.

[24] European Committee for Standardization (CEN) (2020) prEN 1993-1-1. *Eurocode 3: Design of Steel Structures – Part 1-4: General Rules and Rules for Buildings*. Final Document. Brussels, Belgium.

[25] American Society of Civil Engineers (ASCE) (2016) ASCE 7. *Minimum design loads and associated criteria for buildings and other structures*. Virginia, USA.

[26] Standards Australia (AS/NZS) (2002) AS/NZS 1170.0. *Structural design actions, Part 0: General principles*. Sydney, Australia.

[27] Associació Française de Normalització (AFNOR) (2013) NF EN 1993-1-1/NA. *National Annex to Eurocode 3: Design of Steel Structures – Part 1-1: General Rules and Rules for Buildings*. La Plaine Saint-Denis, France.

[28] Kitipornchai, S.; Blinco, L.W.; Grummitt, S.E. (1991) *Portal frame design charts. Australian Institute of Steel Construction (AISC)*. First edition. Australia.

[29] Woolcock, S.T.; Kitipornchai, S.; Bradford, M.A.; Haddad, G.A. (2011) *Design of portal frame buildings including crane runway beams and monorails*. Australian Steel Institute (ASI). Fourth edition. Australia.

[30] Ellingwood, B.R. (1989) *Serviceability Guidelines for Steel Structures*. Engineering Journal (AISC) 26, 1–8.

[31] Comisión Permanente de Estructuras de Acero (2012) EAE *Instrucción de Acero Estructural*. Madrid, Spain.

[32] Arrayago, I.; Real, E.; Gardner, L. (2015) *Description of stress-strain curves for stainless steel alloys*. Materials & Design 87, 540–552.

[33] Steel Construction Institute (SCI) (2017) *Design Manual for Structural Stainless Steel*. Fourth Edition. UK.

[34] European Committee for Standardization (CEN) (2009) EN 10088-4. *Stainless Steels Part 4: Technical Delivery Conditions for Sheet/Plate and Strip of Corrosion Resisting Steels for Construction Purposes*. Brussels, Belgium.

[35] Rossi, B.; Afshan, S; Gardner, L. (2013) *Strength enhancements in cold-formed structural sections – Part II: Predictive models*. Journal of Constructional Steel Research 83, 189–196.

[36] European Committee for Standardization (CEN) (2018) EN 1090-2:2018. *Execution of steel structures and aluminium structures. Technical requirements for steel structures*. Brussels, Belgium.

[37] Gardner, L.; Nethercot, D.A. (2004) *Numerical modelling of stainless steel structural components - A consistent approach*. Journal of Structural Engineering *(ASCE)* 130(10), 1586–1601.

[38] Shayan, S.; Rasmussen, K.J.R.; Zhang, H. (2014) *On the modelling of initial geometric imperfections of steel frames in advanced analysis*. Journal of Constructional Steel Research 98, 167–177.

[39] Arrayago, I.; Rasmussen, K.J.R. (2022) *Influence of the imperfection direction on the ultimate response of steel frames in advanced analysis*. Journal of Constructional Steel Research 190, 107137.

[40] Gardner, L.; Cruise, R.B. (2009) *Modeling of residual stresses in structural stainless steel sections*. Journal of Structural Engineering (ASCE) 135(1), 42–53.

[41] ABAQUS. (2010) Version 6.10. Simulia, Dassault Systèmes, France.

[42] Rasmussen, K.J.R.; Hancock, G.J. (1993) *Design of cold-formed stainless steel tubular members. I: Columns*. Journal of Structural Engineering (ASCE) 119(8), 2349–2367.

[43] Liu, W.; Rasmussen, K.J.R.; Zhang, H. (2017) *Modelling and probabilistic study of the residual stress of cold-formed hollow steel sections*. Engineering Structures 150, 986–995.

[44] Rosson, B.T. (2018) *Modeling the Influence of Residual Stress on the Ultimate Load Conditions of Steel Frames*. Proceedings of the Annual Stability Conference, Structural Stability Research Council. Baltimore, Maryland.

[45] Walport, F.; Gardner, L.; Nethercot, D.A. (2020) *Equivalent bow imperfections for use in design by second order inelastic analysis*. Structures 26, 670–685.

[46] European Committee for Standardization (CEN) (2005) EN 1993-1-8. *Eurocode 3: Design of Steel Structures – Part 1-8: Design of joints*. Brussels, Belgium.

[47] Fieber, A.; Gardner, L.; Macorini, L. (2019) *Formulae for determining elastic local buckling half-wavelengths of structural steel cross-sections*. Journal of Constructional Steel Research 159, 493–506.

[48] European Committee for Standardization (CEN) (2020) prEN 1993-1-5. *Eurocode 3: Design of Steel Structures – Part 1-5: Plated structural elements*. Final Document. Brussels, Belgium.

[49] Gardner, L., Fieber, A. and Macorini, L. (2019) *Formulae for calculating elastic local buckling stresses of full structural cross-sections*. Structures 17, 2–20.

[50] Li, Z. and Schafer, B.W. (2010) *Buckling analysis of cold-formed steel members with general boundary conditions using CUFSM: conventional and constrained finite strip methods*. Twentieth International Speciality Conference on Cold-Formed Steel Structures. Saint Louis, USA.

[51] Walport, F.; Arrayago, I.; Gardner, L.; Nethercot, D.A. (2021) *Influence of geometric and material nonlinearities on the behaviour and design of stainless steel frames*. Journal of Constructional Steel Research 187, 106981.

[52] European Committee for Standardization (CEN) (2002) EN 1991-1-1. *Eurocode 1: Actions on structures – Part 1-1: General actions. Densities, self-weight, imposed loads for buildings*. Brussels, Belgium.

[53] European Committee for Standardization (CEN) (2005) EN 1991-1-4. *Eurocode 1: Actions on structures – Part 1-4: Wind Actions*. Final Document. Brussels, Belgium.